
Interventional Imbalanced Multi-Modal Representation Learning via β -Generalization Front-Door Criterion

Yi Li*
 UCAS[†] & ISCAS[‡]
 liyitunan@gmail.com

Jiangmeng Li[✉]*
 ISCAS
 jiangmeng2019@iscas.ac.cn

Fei Song
 UCAS & ISCAS
 songfei2022@iscas.ac.cn

Qingmeng Zhu
 ISCAS
 qingmeng@iscas.ac.cn

Changwen Zheng
 ISCAS
 changwen@iscas.ac.cn

Wenwen Qiang
 ISCAS
 qiangwenwen@iscas.ac.cn

Abstract

Multi-modal methods establish comprehensive superiority over uni-modal methods. However, the *imbalanced* contributions of different modalities to task-dependent predictions constantly degrade the discriminative performance of canonical multi-modal methods. Based on the contribution to task-dependent predictions, modalities can be identified as *predominant* and *auxiliary* modalities. Benchmark methods raise a tractable solution: augmenting the auxiliary modality with a minor contribution during training. However, our empirical explorations challenge the fundamental idea behind such behavior, and we further conclude that benchmark approaches suffer from certain defects: insufficient theoretical interpretability and limited exploration capability of discriminative knowledge. To this end, we revisit multi-modal representation learning from a causal perspective and build the Structural Causal Model. Following the empirical explorations, we determine to capture the true causality between the discriminative knowledge of predominant modality and predictive label while considering the auxiliary modality. Thus, we introduce the β -generalization front-door criterion. Furthermore, we propose a novel network for sufficiently exploring multi-modal discriminative knowledge. Rigorous theoretical analyses and various empirical evaluations are provided to support the effectiveness of the innate mechanism behind our proposed method.

1 Introduction

Background. A fundamental idea behind multi-modal representation learning (MML) is that the multiple modalities provide comprehensive information from different aspects, e.g., data collected from various sensors, which is inspired by the multi-sensory integration ability of humans [55]. Recent advances in MML [57, 58, 22, 61] demonstrate that multiple modalities can indeed promote

*Contributed equally (Jiangmeng Li is the corresponding author).

[†]University of Chinese Academy of Sciences.

[‡]Institute of Software Chinese Academy of Sciences.

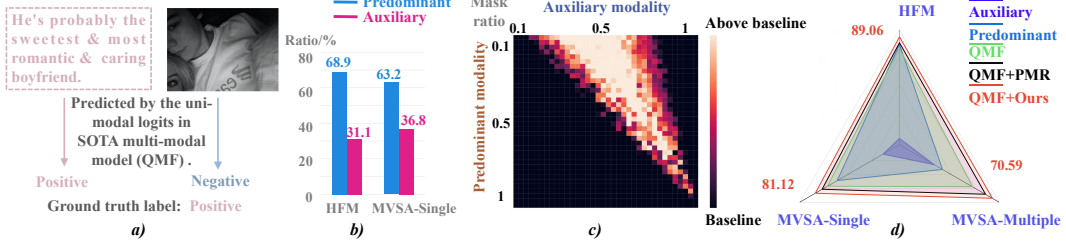


Figure 1: a): We provide an example in the MVSA-Single dataset. Concretely, we utilize the uni-modal logits in the state-of-the-art (SOTA) multi-modal method QMF [54] to get uni-modal predictions. The emotion in the text is predicted as positive, while that of the image is predicted as negative. b): On the two multi-modal datasets (HFM and MVSA-Single, in which text is predominant and image is auxiliary), our statistical results indicate that, in cases where the predicted labels from the predominant and auxiliary modalities are inconsistent, the ratio that label predicted by the predominant modality is identical with the ground truth label significantly exceeds that of the auxiliary modality. c): When evaluating the performance of QMF, we freeze all parameters of QMF and mask specific dimensions of the latent multi-modal features randomly under different ratios. We plot the performance as the heatmap, in which the lighter the color, the greater the performance boosts. d): We depict the experimental results of various MML methods. The results demonstrate that solely utilizing the *predominant* modality outperforms solely utilizing the *auxiliary* modality. QMF leverages both the predominant and auxiliary modalities to achieve further performance improvement. PMR [20] is an AMEM. *QMF+PMR* augments the auxiliary modality in QMF and outperforms the plain QMF, while *QMF+Ours* achieves superior performance compared to *QMF+PMR*.

multi-modal models to achieve significant performance superiority over uni-modal approaches in various fields, e.g., knowledge graph [62, 63], recommendation system [64, 65], sentiment analysis [66, 68], and so on.

Challenge. However, canonical MML approaches [68, 43, 66] generally overlook the imbalance of different modalities, i.e., they assume that the contributions of different modalities toward the prediction of the downstream tasks are approximately balanced. Yet the theoretical and empirical basis behind such an assumption is fragile, and we conduct experimental explorations to support our statement. As shown in Figure 1 a), we provide a specific illustrative example to demonstrate that the label consistency is divergent among different modalities, such that the prediction contributions of modalities are *imbalanced*. As shown in Figure 1 b), the statistical results on the real-world datasets further prove the correctness of the above statement. Therefore, equally leveraging different modalities in MML degrades the model performance of learning discriminative knowledge.

To address the performance degeneration of MML incurred by the imbalanced multiple modalities, the auxiliary modality enhancement methods (AMEMs) [22, 20, 16] propose to augment the auxiliary modality during the training process, which is based on the idea that the major contribution of the predominant modality leads to the insufficient learning of the auxiliary modality. However, the exploration of existing benchmark methods from the dimensional perspective contradicts the behavior of the AMEMs. As depicted in Figure 1 c), masking the dimensions of multi-modal features randomly with a certain ratio leads to performance boosts, which are consistently observed in the upper triangular region of the heatmap. This observation means that compared to the predominant modality, masking more dimensions of the auxiliary features introduces better performance boosts, which is opposite to the AMEMs’ behavior (augmenting the auxiliary modality). Therefore, such a contradictory phenomenon demonstrates the lack of theoretical interpretability in AMEMs. Furthermore, masking the dimensions of multi-modal features leads to performance boosts, which proves the existence of noisy information detrimental to the downstream task. Thus, the discriminative knowledge explored by benchmark MML methods still has the potential to be improved.

Methodology. To this end, we revisit MML from the causal perspective. Theoretically, without loss of generality, we propose a Structural Causal Model (SCM) [45, 46, 47] to declare the intrinsic mechanism of introducing multiple modalities to acquire performance improvement. From our empirical observations in Figure 1 b) and Figure 1 c), we derive an inductive conclusion: the task-dependent discriminative knowledge contained in predominant modality is superior to that of auxiliary modality, and the auxiliary modality may have certain label-inconsistent noisy information, such that *naively* combining multiple modalities cannot achieve the most significant performance boosts

for MML models. Figure 1 d) provides sufficient evidence for the proposed inductive conclusion. From the empirical results in Figure 1 d), we further observe that considering the auxiliary modality, the MML model can better explore the discriminative knowledge. In this regard, according to the proposed SCM for MML, we enable the MML methods to explore the *true causality* between the discriminative knowledge of the predominant modality and the ground truth label during the training process while considering the auxiliary modality. Thus, we introduce the β -generalization front-door criterion and deduce the corresponding adjustment formula from the joint distribution decomposition perspective. To better describe the intuition behind the β -generalization front-door criterion, we provide the theoretical analysis from the multi-world symbolic deduction perspective. Following the understanding of our theoretical findings, we implement a novel *Interventional imbalanced Multi-Modal representation Learning* method for general MML, dubbed *IMML*, which further improves the ability of MML methods in exploring discriminative knowledge from multiple modalities. Theoretically, we provide sufficient support and proof to confirm the correctness and effectiveness of IMML. In practice, the proposed IMML can function as a plug-and-play component to improve the MML performance within the imbalanced scenario. We conduct abundant empirical experiments to demonstrate the effectiveness of IMML consistently.

Contribution. Our major contribution is four-fold: **i)** We conduct empirical explorations to demonstrate the long-standing defects challenging SOTA MML methods: the insufficient theoretical interpretability and the limited ability to extract modality discriminative knowledge. **ii)** From the causal perspective, we theoretically propose a SCM to understand the intrinsic mechanism behind MML. To capture the true causality between the discriminative knowledge of the predominant modality and the predictive label while considering the auxiliary modality, we introduce the β -generalization front-door criterion and provide the corresponding adjustment formula with complete deduction. **iii)** Inspired by empirical exploration, we propose a novel network for sufficiently exploring discriminative knowledge from multiple modalities. **iv)** We propose IMML, which consists of the above two modules. Furthermore, this paper provides rigorous theoretical analyses and sufficient empirical evaluations to support the effectiveness of the innate mechanism behind IMML.

2 Related Works

Multi-modal representation learning. MML aims to integrate modality-specific features to obtain a joint representation for downstream tasks. Canonical MML methods treat each modality equally. For example, Self-MM [43] learns the multi-modal features by self-supervised learning, and CLMLF [66] leverages the intrinsic attention mechanism of Transformer [67] to execute the multi-modal fusion. Noting the imbalanced contributions of different modalities, AMEMs make great progress, e.g., the gradient modulation in OGM [22], the prototypical method in PMR [20] and the modality knowledge distillation in UMT [16] are proposed to augment the auxiliary modality during the training process. However, AMEMs suffer from a lack of theoretical interpretability and a limited ability to explore discriminative knowledge. This paper addresses these two defects by proposing IMML, a new MML paradigm for the imbalanced scenario.

Causal inference. Because of its ability to eliminate the harmful bias of confounders and discover the causality between multiple variables [45], causal inference boosts the development of artificial intelligence [41, 40, 39]. A widely used approach is *intervention* [30, 37, 38, 31]. For example, based on the proposed SCM, ICL-MSR [37] introduces a regularization term to mitigate background disturbances through backdoor adjustment, and D&R [38] utilizes knowledge distillation to leverage external semantic knowledge from the causal perspective. However, performing causal intervention via the front-door criterion has been sparsely explored [4, 3], and these approaches adhere to the standard constraints (three principles introduced in [45]) to execute front-door adjustment. IMML is the pioneering work to introduce the β -generalization front-door criterion. Guided by this criterion, front-door adjustment can be executed under lenient constraints (satisfying two out of three principles).

3 Revisiting the Imbalanced MML from the Causal Perspective

We propose building an SCM [46, 47] to comprehensively understand the intrinsic mechanism behind the imbalanced MML.

3.1 Structural Causal Model

Following the observational exploration in **Section 1**, i.e., the existence of the predominant modality and the presence of the confounding factors in the learned representations, we build the SCM as demonstrated in Figure 2 a), which holds due to the following reasons:

i) $K_P \rightarrow Y \leftarrow K_A$. K_P and K_A denote the complete knowledge of the predominant modality P and the auxiliary modality A in the MML, respectively. Y denotes the corresponding predictive label. As the fundamental assumption of MML [48, 49, 50, 61], the knowledge of multiple modalities contains the task-dependent information, such that Y is determined by K_P and K_A via two decoupled ways: the direct $K_P \rightarrow Y$ and $K_A \rightarrow Y$. It is worth noting that modeling the complete knowledge of K_P and K_A is unachievable for two reasons: i) the candidate inputs are sampled from the complete domain of a modality so that the available knowledge is *incomplete*; ii) the knowledge modeling process is canonically performed by leveraging a non-linear neural network encoder, while according to the data processing inequality [52, 51], a certain inconsistency generally exists between the original knowledge of a specific modality and the corresponding modeled knowledge. Thus K_P and K_A are determined as unknown in the SCM. **ii) $K_P \rightarrow D_P \rightarrow Z \rightarrow Y$ and $K_A \rightarrow D_A \rightarrow Z \rightarrow Y$.** We use D_P to represent the discriminative knowledge extracted by the encoder from the complete knowledge of the predominant modality. Similarly, D_A signifies the discriminative knowledge gleaned from the complete knowledge of auxiliary modality. Z presents the ultimate multi-modal representation formed by fusing D_P and D_A . We reckon that Y is further jointly determined by K_P and K_A via the mediation ways, including $K_P \rightarrow D_P \rightarrow Z \rightarrow Y$ and $K_A \rightarrow D_A \rightarrow Z \rightarrow Y$. Specifically, the reasons behind the above statement include:

1) $K_P \rightarrow D_P$ and $K_A \rightarrow D_A$: the discriminative knowledge D_P and D_A are extracted from K_P and K_A by the neural network-based encoders in MML, and the intuition behind the behavior is to model task-dependent information from multiple modalities for the prediction of Y ; 2) $D_P \rightarrow Z \leftarrow D_A$: the multi-modal representation Z is obtained by fusing the uni-modal representations, which contains the modal-specific discriminative knowledge, i.e., D_P and D_A ; 3) $Z \rightarrow Y$: this can be implemented by the target mapping, which bridges the latent space and target space (e.g., the target mapping can be the classification layer).

3.2 β -Generalization Front-Door Criterion

By observing the empirical explorations in Figure 1 b) and Figure 1 c), we determine that encouraging the multi-modal representation to focus on modeling the discriminative knowledge of the predominant modality can significantly improve the performance of MML methods. To profoundly understand the phenomenon, we further analyze the experimental results in Figure 1 d) and find: i) the existence of a predominant modality generally holds in MML, since learning representations solely from a certain modality consistently outperforms learning from another modality; ii) appropriately leveraging the auxiliary modality can significantly improve the model to learn task-dependent discriminative knowledge. Specifically, we conclusively determine that with the assistance of introducing the auxiliary modality, prompting the model to learn the causal effect between the discriminative knowledge of the predominant modality and the predictive label can improve the MML performance. By incorporating the above conclusion into the proposed SCM in Figure 2 a), we propose sufficiently capturing the causal effect between D_P and Y while considering D_A .

In this regard, we revisit the SCM from the causal intervention perspective. For ease of understanding, we introduce the following definitions:

Definition 3.1. (α back-door path.) Regard A and B as the candidate elements within a front-door criterion scenario, and the α back-door path *directly* interferes with the estimation of the causality between A and B .

As shown in Figure 2 b), the back-door path $Y \leftarrow K_P \rightarrow D_P$, interfering with the estimation of the causality between D_P and Y , is a canonical embodiment of Definition 3.1.

Definition 3.2. (β back-door path.) Regard A and B as the candidate elements, and C is a *mediator* between A and B within a front-door criterion scenario. The β back-door path *indirectly* interferes with the estimation of the causality between A and B via the mediator C .

As shown in Figure 2 b), the back-door path $Y \leftarrow K_A \rightarrow D_A \rightarrow Z$, which interferes with the estimation of the causality between D_P and Y via the mediator Z , exemplifies Definition 3.2.

The causal sub-graph, containing K_P , D_P , Z , and Y , well fits the conditions of the canonical front-door criterion [46, 47], which only includes a single back-door path between D_P and Y , i.e., α back-door path, but the existence of β back-door path violates one of the conditions of the front-door criterion, i.e., “**all backdoor paths from Z to Y should be blocked by D_P** ” [46, 47]. Inspired by causal applications in various fields [1, 2], we propose introducing the β -generalization front-door criterion for our proposed SCM.

3.3 Causal Intervention via the Joint Distribution Decomposition

In this subsection, we propose to perform the causal intervention towards the introduced SCM within the β -generalization front-door criterion scenario, thereby exploring the true causal effects between D_P and Y , i.e., $P(Y|do(D_P = d_p))$. Formally, we present the β -generalization front-door adjustment for the proposed SCM from the perspective of the joint distribution. According to the SCM in Figure 2 b), we formalize the corresponding joint distribution as follows:

$$P(D_P, D_A, Z, K_A, K_P, Y) = P(K_A)P(K_P)P(D_A|K_A)P(D_P|K_P)P(Z|D_A, D_P)P(Y|Z, K_A, K_P). \quad (1)$$

The $do(\cdot)$ operator removes the connections between the variable to be intervened and its parent nodes in SCM [46], and following our intuition, i.e., introducing $do(D_P = d_p)$, we perform the intervention on Equation 1 by

$$P(K_P, Z, D_A, K_A, Y|do(D_P = d_p)) = P(K_A)P(K_P)P(D_A|K_A)P(Z|D_A, D_P = d_p)P(Y|Z, K_A, K_P),$$

where introducing $do(D_P = d_p)$ is equivalent to removing the term $P(D_P|K_P)$. The objective is to ascertain the causal impact of D_P on Y . Therefore, we aggregate over the variables Z, K_P, K_A, D_A :

$$P(Y|do(D_P = d_p)) = \sum_Z \sum_{K_P} \sum_{K_A} \sum_{D_A} P(Z|D_P = d_p, D_A)P(D_A|K_A)P(K_A)P(K_P)P(Y|Z, K_A, K_P). \quad (2)$$

As outlined in Section 3.1, K_P, K_A represent the complete knowledge from the predominant and auxiliary modalities, respectively. Given that K_P, K_A are unknown, it is necessary to exclude K_P, K_A from Equation 2. With this intuition, we introduce the following deduction:

$$\begin{aligned} & \sum_Z \sum_{K_P} \sum_{K_A} \sum_{D_A} P(Y|K_P, K_A, Z)P(D_A|K_A)P(K_A)P(K_P)P(Z|D_P = d_p, D_A) \\ &= \sum_Z \sum_{K_P} \sum_{K_A} \sum_{D_A} \sum_{d'_p \in D_P} P(Y|K_P, K_A, Z)P(K_P|D_P = d'_p)P(D_P = d'_p)P(Z|D_P = d_p, D_A) \end{aligned} \quad (3a)$$

$$P(D_A|K_A)P(K_A) \quad (3a)$$

$$= \sum_Z \sum_{K_A} \sum_{D_A} \sum_{d'_p \in D_P} \sum_{K_P} P(Y|K_P, K_A, Z, D_P = d'_p)P(K_P|D_P = d'_p, Z, K_A)P(D_P = d'_p)P(D_A|K_A) \quad (3b)$$

$$P(K_A)P(Z|D_P = d_p, D_A) \quad (3b)$$

$$= \sum_Z \sum_{K_A} \sum_{D_A} \sum_{d'_p \in D_P} P(Y|K_A, Z, D_P = d'_p)P(D_P = d'_p)P(K_A|D_A)P(D_A)P(Z|D_P = d_p, D_A) \quad (3c)$$

$$= \sum_Z \sum_{D_A} \sum_{d'_p \in D_P} \sum_{K_A} P(Y|K_A, Z, D_P = d'_p, D_A)P(K_A|D_A, Z, D_P = d'_p)P(Z|D_P = d_p, D_A) \quad (3d)$$

$$P(D_P = d'_p)P(D_A) \quad (3e)$$

$$= \sum_Z \sum_{D_A} \sum_{d'_p \in D_P} P(Y|Z, D_P = d'_p, D_A)P(Z|D_P = d_p, D_A)P(D_P = d'_p)P(D_A). \quad (3f)$$

(3a) holds due to the application of the total probability equation; (3b) holds because Y is independent of D_P given K_P, K_A, Z and K_P is independent of Z, K_A given D_P ; (3c) holds due to the application

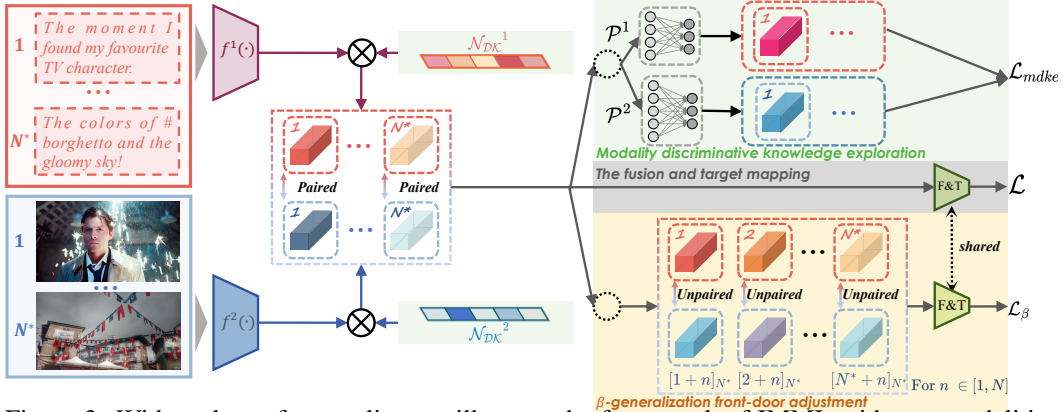


Figure 3: Without loss of generality, we illustrate the framework of IMML with two modalities, i.e., text and image. The green and yellow boxes represent the modality discriminative knowledge exploration module and the β -generalization front-door adjustment module. $F\&T$ stands for the fusion and target mapping module of arbitrary multi-modal models. Therefore, IMML can be treated as a plug-and-play component to boost the performance of MML within the imbalanced scenario.

of the total probability equation given D_P, Z, K_A (the red term in (3b); (3d) holds due to the Bayes equation (i.e., $P(K_A|D_A) = \frac{P(D_A|K_A)P(K_A)}{P(D_A)}$); (3e) holds because Y is independent of D_A given K_A, Z, D_P and K_A is independent of Z, D_P given D_A ; (3f) holds due to the application of the total probability equation given D_P, D_A, Z (the blue term in (3e)). To better demonstrate the intuition behind the behavior of β -generalization front-door adjustment, we provide the theoretical analysis from the *multi-world symbolic deduction* perspective in [Appendix A.1](#). Accordingly, we implement our methodology by adhering to the proposed causal intervention upon the SCM.

4 Methodology

We provide an illustrative architecture of IMML in Figure 3. IMML introduces a modality discriminative knowledge exploration network to discern D_P and D_A from K_P and K_A . IMML also provides a detailed functional implementation for the β -generalization front-door adjustment described.

4.1 Modality Discriminative Knowledge Exploration

Formally, given a minibatch of multi-modal samples $\mathcal{X} = \{(x_i^m, y_i) | i \in [1, \dots, N^*], m \in [1, \dots, M]\}$, where N^* and M denote the batch size and the number of modalities, respectively. Specifically, the sample x_i^m is first fed into the m -th modality-specific encoder f^m (e.g., BERT [6] for text) to obtain corresponding uni-modal feature $h_i^m = f^m(x_i^m)$. Then we build a learnable modality discriminative knowledge exploration network $\mathcal{N}_{DK}^m = \{\omega_k^m | k \in [1, \dots, D_m]\}$, where D_m is the dimension of m -th modality's latent feature. \mathcal{N}_{DK}^m assigns a weight to each dimension of the representation h_i^m by $\hat{h}_i^m = h_i^m \otimes \mathcal{N}_{DK}^m$, where $\hat{h}_i^m \in \mathbb{R}^{D_m}$ denotes the extracted discriminative feature of the m -th modality and \otimes is an element-wise Hadamard product function. Generally, the latent features of M modalities have various dimensions, posing challenges in calculating the modality discriminative knowledge exploration loss. In this regard, we employ a projection head $\mathcal{P}^m : \mathbb{R}^{D_m} \rightarrow \mathbb{R}^D$ to obtain the dimensional-consistent latent multi-modal features $\xi_i^m = \mathcal{P}^m(\hat{h}_i^m)$, where $\xi_i^m \in \mathbb{R}^D$. Then the loss of the modality discriminative knowledge exploration network can be formalized as

$$\mathcal{L}_{mdke} = \sum_{m=1}^M \mathcal{L}_{mdke}^{m, [m+1]_M}, \quad (4)$$

where $[x]_n = \begin{cases} x & \text{if } 1 \leq x \leq n \\ x \bmod n & \text{if } x > n \end{cases}$ and

$$\mathcal{L}_{mdke}^{m, [m+1]_M} = - \sum_{i=1}^{N^*} \log \frac{\exp[d(\xi_i^m, \xi_i^{[m+1]_M})/\tau]}{\sum_{i'=1}^{N^*} \sum_{m'=m'} \mathbb{I}_{[i \neq i' \vee m \neq m']} \exp[d(\xi_i^m, \xi_{i'}^{m'})/\tau]}, \quad (5)$$

where $m' \in \{m, [m+1]_M\}$, $d(\cdot)$ is a similarity measuring function implemented by Cosine similarity, $\mathbb{I}_{[i \neq i' \vee m \neq m']}$ denotes an indicator function equalling to 1 if $i \neq i'$ or $m \neq m'$, and τ is a

temperature parameter valued by following [21]. \mathcal{L}_{mdke} is a variant of contrastive loss [21, 17], and we train $\mathcal{N}_{\mathcal{DK}}$ using \mathcal{L}_{mdke} because canonical supervised loss, e.g., cross-entropy loss [19], can only measure the *empirical error*, whereas the introduced \mathcal{L}_{mdke} can well bound the *generalization error* for MML, as demonstrated by Theorem 5.2. Therefore, by minimizing \mathcal{L}_{mdke} , we can improve the generalizability of our method, thus enhancing the ability of MML models to capture discriminative knowledge from multiple modalities.

4.2 β -Generalization Front-Door Adjustment

This section introduces the implemented loss function for the β -generalization front-door adjustment. Without loss of generality, let $\mathcal{F}[\cdot, \cdot]$ be the arbitrary multi-modal fusion operation (e.g., $\mathcal{F}[\cdot, \cdot]$ can be concatenation, weighted summation, and so on). Let P and A represent the predominant and auxiliary modality, respectively. Then the dataset can be simplified as $\mathcal{X} = \{(x_i^m, y_i) | i \in [1, \dots, N^*], m \in \{P, A\}\}$. As mentioned in Section 4.1, we can denote the discriminative knowledge of predominant and auxiliary modalities by $\{\hat{h}_i^m | i \in [1, \dots, N^*], m \in [P, A]\}$. Given $D_P = \hat{h}_i^p$ and Equation 3, $P(Y|do(D_P = \hat{h}_i^p))$ can be rewritten as

$$\begin{aligned} & \sum_Z \sum_{i''=1}^{N^*} \sum_{i'=1}^{N^*} P(Y|Z, D_P = \hat{h}_{i''}^p, D_A = \hat{h}_{i'}^a) P(D_P = \hat{h}_{i''}^p) P(Z|D_P = \hat{h}_i^p, D_A = \hat{h}_{i'}^a) P(D_A = \hat{h}_{i'}^a) \\ &= \sum_Z \sum_{i', i''=1}^{N^*} P(Y|Z, \hat{h}_{i''}^p, \hat{h}_{i'}^a) P(\hat{h}_{i''}^p) P(Z|\hat{h}_i^p, \hat{h}_{i'}^a) P(\hat{h}_{i'}^a). \end{aligned} \quad (6)$$

Therefore, we have transformed the summation over D_P and D_A into the summation over the discriminative features of the predominant and auxiliary modality. Theoretically, following the computation of Equation 6, we disclose that the calculation of $P(Z|\hat{h}_i^p, \hat{h}_{i'}^a)$ necessitates matching \hat{h}_i^p with each $\hat{h}_{i'}^a$. To avoid the excessive computation complexity, we propose to match \hat{h}_i^p with those whose indexes are close to \hat{h}_i^p . Specifically, given $D_P = \hat{h}_i^p$, we have $i' \in \{[i+1]_{N^*}, \dots, [i+N]_{N^*}\}$, where N is the hyper-parameter and $[\cdot]_{N^*}$ ensures $1 \leq i' \leq N^*$. With the intuition to fuse unpaired multi-modal features (predominant feature \hat{h}_i^p and its mismatched/unpaired features $\hat{h}_{i'}^a$), we innovatively implement

$$z(\hat{h}_i^p, \hat{h}_{i'}^a) = z(\hat{h}_i^p, \hat{h}_{i'}^{a^1}, \hat{h}_{i'}^{a^2}, \dots, \hat{h}_{i'}^{a^{M-1}}) = \mathcal{F}\left[\lambda \hat{h}_i^p, \frac{(1-\lambda)\hat{h}_{i'}^{a^1}}{M-1}, \frac{(1-\lambda)\hat{h}_{i'}^{a^2}}{M-1}, \dots, \frac{(1-\lambda)\hat{h}_{i'}^{a^{M-1}}}{M-1}\right].$$

To ensure $0 \leq \lambda \leq 1$, we sample λ from Beta-distribution [42, 33], i.e., $\lambda \sim Beta(\alpha, \beta)$, where α and β are two hyper-parameters. Meanwhile, the ground truth label of feature $z(\hat{h}_i^p, \hat{h}_{i'}^a)$ is intuitively inconsistent with the labels of x_i^p or $x_{i'}^a$. Thus, we redefine the ground truth label of $z(\hat{h}_i^p, \hat{h}_{i'}^a)$ by $Y_z = Y[z(\hat{h}_i^p, \hat{h}_{i'}^{a^1}, \hat{h}_{i'}^{a^2}, \dots, \hat{h}_{i'}^{a^{M-1}})] = \lambda y(\hat{h}_i^p) + \frac{1}{M-1} \sum_{m=1}^{M-1} (1-\lambda)y(\hat{h}_{i'}^{a^m})$. Overall, in Equation 6, we have $P(D_A = \hat{h}_{i'}^a) = \frac{1}{N}$, $P(D_P = \hat{h}_{i''}^p) = \frac{1}{N^*}$, and

$$P(Z|\hat{h}_i^p, \hat{h}_{i'}^a) = \begin{cases} \frac{1}{NN^*}, & \text{if } Z = z(\hat{h}_i^p, \hat{h}_{i'}^a) \\ 0, & \text{else} \end{cases}. \quad (7)$$

According to the definition of i' , we derive the following result: $P(Y|Z, \hat{h}_{i''}^p, \hat{h}_{i'}^a) = 0$ if $i'' \neq i$. Then, $P(Y|Z, \hat{h}_{i''}^p, \hat{h}_{i'}^a) = P(Y_z|Z = z(\hat{h}_i^p, \hat{h}_{i'}^a))$, thus resulting in $P(Y|do(D_P = \hat{h}_i^p)) = \frac{1}{C} \sum_{i'} P(Y_z|Z = z(\hat{h}_i^p, \hat{h}_{i'}^a))$, where C is the constant term about the probability. To capture the true causality between D_P and Y , we determine to maximize $P(Y|do(D_P = d_p))$, i.e., minimizing the following loss function for a minibatch of multi-modal samples:

$$\mathcal{L}_\beta = \sum_{i=1}^{N^*} \sum_{i'=[i+1]_{N^*}}^{[i+N]_{N^*}} l(Y_z, z(\hat{h}_i^p, \hat{h}_{i'}^a)), \quad (8)$$

where $l(\cdot)$ is the loss function of the downstream task, e.g., $l(\cdot)$ can be the cross-entropy loss [19], mean squared error [18], and so on. By performing the multi-task learning [15], we acquire the loss function of IMML as follows:

$$\mathcal{L}_{imml} = \gamma_1 \mathcal{L}_{mdke} + \gamma_2 \mathcal{L}_\beta + \mathcal{L}, \quad (9)$$

where γ_1 and γ_2 are two hyper-parameters that control the influence of \mathcal{L}_{mdke} and \mathcal{L}_β , respectively. \mathcal{L} denotes the loss function of arbitrary benchmark MML methods, making IMML a plug-and-play component that can be generally implemented to improve various benchmarks. The overall training pipeline is depicted in Appendix A.2.

5 Theoretical Analysis on Generalization Error Bound

We confirm that the generalization error of MML is well bounded by \mathcal{L}_{mkde} with rigorous theoretical proofs. To present the connection between the generalization error and \mathcal{L}_{mkde} , we introduce a fundamental assumption:

Assumption 5.1. (Uni-modal label consistency in MML). Suppose that the labels of paired uni-modal data are identical, i.e., $\forall m_1, m_2 \in [1, \dots, M], Y(x_i^{m_1}) = Y(x_i^{m_2})$.

Indeed, Assumption 5.1 is practical and can be easily achieved in real-world scenarios. For example, during the data annotation process, only the image and text pairs with consistently assigned labels are retained as data samples in the dataset [27]. Considering that the SOTA multi-modal classification models (MMBT [24], TMC [28], and QMF [54]) employ a linear classification layer as target mapping and use cross-entropy loss function, without loss of generality, we derive the Theorem 5.2 based on the mentioned theoretical condition and the achievable Assumption 5.1.

Theorem 5.2. (*The upper bound of generalization error*). *Let \mathcal{M} be the multi-modal model with a linear classification layer and satisfy the practical Assumption 5.1. Then for a K -class classification task, the generalization error of \mathcal{M} can be bounded by \mathcal{L}_{mdke} :*

$$GError(\mathcal{M}) \leq \sum_{m=1}^M \mathbb{E}(\phi_m) \mathbb{E}[\mathcal{L}_{mdke}(\mathcal{N}f^m(x^m)) + \sqrt{\text{Var}(\mathcal{N}f^m(x^m) | y)} + \mathcal{O}(\sqrt{2N^* - 2}) - \log \frac{2N^* - 2}{K}],$$

where ϕ_m is the weight of the m -th modality in the multi-modal fusion, $\mathcal{N}f^m = \mathcal{N}_{DK}^m \circ f^m$, and $\text{Var}(\mathcal{N}f^m(x^m) | y) = \mathbb{E}_{p(y)} [\mathbb{E}_{p(x^m | y)} \|\mathcal{N}f^m(x^m) - \mathbb{E}_{p(x^m | y)} \mathcal{N}f^m(x^m)\|^2]$.

The proof is provided in **Appendix A.3**. From Theorem 5.2, we are inspired that by minimizing the loss \mathcal{L}_{mdke} , we can reduce the generalization error of the multi-modal model \mathcal{M} , thereby ensuring the performance of \mathcal{M} on unseen data samples.

In summary, the two proposed losses are well-supported theoretically. With the guarantee of causality, minimizing \mathcal{L}_β can explore the true causality between the discriminative knowledge of the predominant modality and the ground truth label while considering the auxiliary modality. According to Theorem 5.2, minimizing \mathcal{L}_{mdke} can enhance the generalizability of MML methods.

6 Experiments

We provide details of the datasets, baselines, and implementations in **Appendix A.4**.

Experimental results. To facilitate comprehensive comparisons, as per the baselines [54, 28], we add Gaussian noise to the images and blank noise to the texts to assess robustness. The overall results are depicted in Table 1, and two salient observations emerge: i) Combined with IMML, benchmark MML methods exhibit significant improvements in classification accuracy, e.g., 3.05% for QMF and 3.85% for L-f on MVSA-Single ($\epsilon = 0$), and 1.66% for QMF on HFM ($\epsilon = 5.0$). We also perform the student t -test [8] to validate the significance of the performance improvement. The results is shown in Table 5 of **Appendix A.5.3**, which confirms that the performance improvement is significant and not due to randomness; ii) Compared to SOTA AMEMs, IMML achieves top-2 performance across four datasets. It's worth noting that UMT utilizes a powerful multi-modal pre-trained model (CLIP [53], which is pre-trained on 400 million pairs of images and texts) to conduct knowledge distillation, thereby improving the learning of features in benchmark MML methods. Therefore, it is probably unfair to compare UMT

Table 2: The extensive link prediction results on two multimodal knowledge graph datasets.

Model	FB-IMG				WN9-IMG			
	MRR	H@1	H@3	H@10	MRR	H@1	H@3	H@10
TransE	0.712	0.618	0.781	0.859	0.865	0.765	0.816	0.871
DistMult	0.706	0.606	0.742	0.808	0.901	0.895	0.913	0.925
ComplEx	0.808	0.757	0.845	0.892	0.908	0.903	0.907	0.928
RotatE	0.794	0.744	0.827	0.883	0.910	0.901	0.915	0.926
TransAE	0.742	0.691	0.785	0.844	0.898	0.894	0.908	0.922
IKLR	0.755	0.698	0.794	0.857	0.901	0.900	0.912	0.928
TBKGE	0.812	0.764	0.850	0.902	0.912	0.904	0.914	0.931
MMKRL	0.827	0.783	0.857	0.906	0.913	0.905	0.917	0.932
OTKGE	0.843	0.799	0.876	0.916	0.923	0.911	0.930	0.947
OTKGE+IMML	0.854	0.812	0.887	0.927	0.930	0.916	0.937	0.955

Table 1: Classification performance of different models. **Red** and **blue** indicate the best and second-best results, respectively. ϵ denotes the noise ratio. The dynamic model means the fusion weights in the multi-modal fusion process are functions of samples rather than constants. \times denotes the multimodal fusion weights are constant, while \checkmark means the weights are the functions of samples.

Model	Food101[23]		MVSA-Single [27]		MVSA-Multiple [27]		HFM [26]	
	$\epsilon = 0.0$	$\epsilon = 5.0$	$\epsilon = 0.0$	$\epsilon = 5.0$	$\epsilon = 0.0$	$\epsilon = 5.0$	$\epsilon = 0.0$	$\epsilon = 5.0$
Bow [25] (\times)	82.50	61.68	48.79	42.20	65.02	54.72	74.95	70.04
ResNet [29] (\times)	64.62	34.72	64.12	49.36	67.08	60.95	75.82	73.53
BERT [6] (\times)	86.46	67.38	75.61	69.50	67.59	64.59	88.09	82.40
L-f [54] (\times)	90.69	68.49	76.88	63.46	66.48	62.20	87.40	83.35
C-Bow [54] (\times)	70.77	38.28	64.09	49.95	66.24	62.45	78.33	75.39
C-BERT [54] (\times)	88.20	61.10	65.59	50.70	67.45	61.95	87.35	81.91
MMBT [6] (\checkmark)	91.52	72.32	78.50	71.99	67.36	64.22	87.25	80.92
TMC [28] (\checkmark)	89.86	73.93	74.88	66.72	68.65	64.82	87.31	83.79
QMF [54] (\checkmark)	92.92	76.03	78.07	73.85	69.40	64.81	87.57	83.90
L-f + PMR [20] (\times)	90.58	68.14	79.38	74.37	70.18	62.18	88.10	85.01
TMC + PMR (\checkmark)	89.72	73.56	77.84	70.33	68.26	64.82	87.51	83.91
QMF + PMR (\checkmark)	92.71	75.07	78.03	71.87	68.77	65.59	88.30	84.60
L-f + UMT [16] (\times)	92.19	75.42	80.85	72.73	69.47	65.71	88.22	85.16
TMC + UMT (\checkmark)	90.94	74.07	77.76	70.99	69.88	66.21	87.55	84.07
QMF + UMT (\checkmark)	93.27	76.01	80.07	74.28	70.53	67.47	88.61	84.88
L-f + IMML (\times)	92.38	75.38	80.73	76.88	70.47	65.64	88.96	84.41
TMC + IMML (\checkmark)	91.30	74.71	77.65	67.24	70.23	66.06	87.46	84.61
QMF + IMML (\checkmark)	93.46	76.31	81.12	74.76	70.59	66.53	89.06	85.56

and IMML. However, for a thorough evaluation, we still compare UMT with IMML and find that IMML outperforms UMT in 7 out of 8 comparisons. Both observations convincingly demonstrate the effectiveness of IMML. To further verify the effectiveness and generalization of IMML, we conduct experiments on two multi-modal knowledge graph datasets encompassing three modalities, and details of the datasets and baselines are provided in [Appendix A.5](#). The results in Table 2 indicate that incorporating IMML enhances the performance of the SOTA method OTKGE on the link prediction task across both datasets.

Table 3: The results of ablation study.

Model	Food101	M-S	M-M	HFM
L-f + IMML w/o \mathcal{L}_{mdke}	91.73	79.96	69.58	88.45
L-f + IMML w/o \mathcal{L}_β	91.47	80.35	69.41	88.36
L-f + IMML	92.38	80.73	70.47	88.96
TMC + IMML w/o \mathcal{L}_{mdke}	90.64	75.92	69.17	87.11
TMC + IMML w/o \mathcal{L}_β	90.86	75.53	68.59	87.36
TMC + IMML	91.30	77.65	70.23	87.46
QMF + IMML w/o \mathcal{L}_{mdke}	93.37	80.15	69.65	88.70
QMF + IMML w/o \mathcal{L}_β	93.29	79.19	70.24	88.41
QMF + IMML	93.46	81.12	70.59	89.06

of leveraging the β -generalization front-door adjustment for learning informative features.

Visual comparison. To intuitively demonstrate the effectiveness of IMML, we visualize the embeddings of test samples on MVSA-Single in Figure 4. Yellow, red, and cyan circles represent the positive, negative, and neutral samples, respectively. The clustering performance shows that IMML effectively clusters intra-class samples tightly while increasing the separation between inter-class samples. Therefore, IMML can help MML methods to learn informative and discriminative features.

Ablation study. Except for the general loss function \mathcal{L} of arbitrary MML methods, IMML consists of two vital loss functions: \mathcal{L}_{mdke} and \mathcal{L}_β . To verify the effectiveness of each component, we conduct the ablation study, and the results are shown in Table 3. We observe that removing any component decreases accuracy, confirming the effectiveness of both \mathcal{L}_{mdke} and \mathcal{L}_β . Moreover, based on the statistics in Table 3, IMML w/o \mathcal{L}_{mdke} outperforms IMML w/o \mathcal{L}_β in two-thirds of cases, confirming the superiority

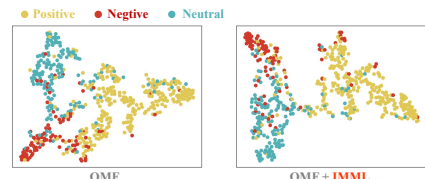


Figure 4: Visualization experiments.

7 Conclusions and Future Discussion

In this paper, we conduct exploratory experiments and derive a conclusion: benchmark MML approaches lack the theoretical interpretability and the ability to capture discriminative knowledge sufficiently from multiple modalities. To better understand MML, we perform the causal analysis and determine to capture the true causality between the discriminative knowledge of predominant modality and task-dependent label while considering the auxiliary modality. To this end, we introduce the β -generalization front-door criterion with the solid theoretical deduction. Furthermore, we propose a novel network to explore modality discriminative knowledge sufficiently. Both theoretical and experimental analyses demonstrate the effectiveness of the proposed IMML. However, the derivation of Theorem 5.2 is based on certain conditions, such as Assumption 5.1, the linear classification layer, and so on. In the future, we aim to derive theories that guide multimodal representation learning under more relaxed constraints. Additionally, applying causal inference to multimodal representation learning has not yet been widely explored. We believe that our proposed paradigm will introduce new perspectives and methods to the community, driving progress in this field.

References

- [1] I. R. Fulcher, I. Shpitser, S. Marealle, and E. J. Tchetgen Tchetgen, “Robust inference on population indirect causal effects: the generalized front door criterion,” *Journal of the Royal Statistical Society Series B: Statistical Methodology*, vol. 82, no. 1, pp. 199–214, 2020.
- [2] H. Jeong, J. Tian, and E. Bareinboim, “Finding and listing front-door adjustment sets,” in *NeurIPS*, 2022.
- [3] ———, “Finding and listing front-door adjustment sets,” *Advances in Neural Information Processing Systems*, vol. 35, pp. 33 173–33 185, 2022.
- [4] L. Xu and A. Gretton, “A neural mean embedding approach for back-door and front-door adjustment,” *arXiv preprint arXiv:2210.06610*, 2022.
- [5] J. Deng, W. Dong, R. Socher, L.-J. Li, K. Li, and L. Fei-Fei, “Imagenet: A large-scale hierarchical image database,” in *2009 IEEE conference on computer vision and pattern recognition*. Ieee, 2009, pp. 248–255.
- [6] J. Devlin, M.-W. Chang, K. Lee, and K. Toutanova, “Bert: Pre-training of deep bidirectional transformers for language understanding,” *arXiv preprint arXiv:1810.04805*, 2018.
- [7] Z. Sun, Z. Deng, J. Nie, and J. Tang, “Rotate: Knowledge graph embedding by relational rotation in complex space,” in *7th International Conference on Learning Representations, ICLR 2019, New Orleans, LA, USA, May 6-9, 2019*. OpenReview.net, 2019. [Online]. Available: <https://openreview.net/forum?id=HkgEQnRqYQ>
- [8] W. Mendenhall, R. J. Beaver, and B. M. Beaver, *Introduction to probability and statistics*. Cengage Learning, 2012.
- [9] H. Mousselly-Sergieh, T. Botschen, I. Gurevych, and S. Roth, “A multimodal translation-based approach for knowledge graph representation learning,” in *Proceedings of the Seventh Joint Conference on Lexical and Computational Semantics*, 2018, pp. 225–234.
- [10] R. Xie, S. Heinrich, Z. Liu, C. Weber, Y. Yao, S. Wermter, and M. Sun, “Integrating image-based and knowledge-based representation learning,” *IEEE Trans. Cogn. Dev. Syst.*, vol. 12, no. 2, pp. 169–178, 2020. [Online]. Available: <https://doi.org/10.1109/TCDS.2019.2906685>
- [11] H. M. Sergieh, T. Botschen, I. Gurevych, and S. Roth, “A multimodal translation-based approach for knowledge graph representation learning,” in *Proceedings of the Seventh Joint Conference on Lexical and Computational Semantics, *SEM@NAACL-HLT 2018, New Orleans, Louisiana, USA, June 5-6, 2018*, M. Nissim, J. Berant, and A. Lenci, Eds. Association for Computational Linguistics, 2018, pp. 225–234. [Online]. Available: <https://doi.org/10.18653/v1/s18-2027>
- [12] Z. Wang, L. Li, Q. Li, and D. Zeng, “Multimodal data enhanced representation learning for knowledge graphs,” in *International Joint Conference on Neural Networks, IJCNN 2019 Budapest, Hungary, July 14-19, 2019*. IEEE, 2019, pp. 1–8. [Online]. Available: <https://doi.org/10.1109/IJCNN.2019.8852079>

[13] B. Yang, W. Yih, X. He, J. Gao, and L. Deng, “Embedding entities and relations for learning and inference in knowledge bases,” in *3rd International Conference on Learning Representations, ICLR 2015, San Diego, CA, USA, May 7-9, 2015, Conference Track Proceedings*, Y. Bengio and Y. LeCun, Eds., 2015. [Online]. Available: <http://arxiv.org/abs/1412.6575>

[14] A. Bordes, N. Usunier, A. García-Durán, J. Weston, and O. Yakhnenko, “Translating embeddings for modeling multi-relational data,” in *Advances in Neural Information Processing Systems 26: 27th Annual Conference on Neural Information Processing Systems 2013. Proceedings of a meeting held December 5-8, 2013, Lake Tahoe, Nevada, United States*, C. J. C. Burges, L. Bottou, Z. Ghahramani, and K. Q. Weinberger, Eds., 2013, pp. 2787–2795.

[15] R. Caruana, “Multitask learning,” *Machine learning*, vol. 28, pp. 41–75, 1997.

[16] C. Du, J. Teng, T. Li, Y. Liu, T. Yuan, Y. Wang, Y. Yuan, and H. Zhao, “On uni-modal feature learning in supervised multi-modal learning,” *arXiv preprint arXiv:2305.01233*, 2023.

[17] Y. Wang, Q. Zhang, Y. Wang, J. Yang, and Z. Lin, “Chaos is a ladder: A new theoretical understanding of contrastive learning via augmentation overlap,” *arXiv preprint arXiv:2203.13457*, 2022.

[18] Z. Wang and A. C. Bovik, “Mean squared error: Love it or leave it? a new look at signal fidelity measures,” *IEEE signal processing magazine*, vol. 26, no. 1, pp. 98–117, 2009.

[19] P.-T. De Boer, D. P. Kroese, S. Mannor, and R. Y. Rubinstein, “A tutorial on the cross-entropy method,” *Annals of operations research*, vol. 134, pp. 19–67, 2005.

[20] Y. Fan, W. Xu, H. Wang, J. Wang, and S. Guo, “Pmr: Prototypical modal rebalance for multimodal learning,” in *Proceedings of the IEEE/CVF Conference on Computer Vision and Pattern Recognition*, 2023, pp. 20 029–20 038.

[21] T. Chen, S. Kornblith, M. Norouzi, and G. Hinton, “A simple framework for contrastive learning of visual representations,” in *International conference on machine learning*. PMLR, 2020, pp. 1597–1607.

[22] X. Peng, Y. Wei, A. Deng, D. Wang, and D. Hu, “Balanced multimodal learning via on-the-fly gradient modulation,” in *Proceedings of the IEEE/CVF Conference on Computer Vision and Pattern Recognition*, 2022, pp. 8238–8247.

[23] X. Wang, D. Kumar, N. Thome, M. Cord, and F. Precioso, “Recipe recognition with large multimodal food dataset,” in *2015 IEEE International Conference on Multimedia & Expo Workshops, ICME Workshops 2015, Turin, Italy, June 29 - July 3, 2015*. IEEE Computer Society, 2015, pp. 1–6.

[24] D. Kiela, S. Bhooshan, H. Firooz, and D. Testuggine, “Supervised multimodal bitransformers for classifying images and text,” in *Visually Grounded Interaction and Language (ViGIL), NeurIPS 2019 Workshop, Vancouver, Canada, December 13, 2019*, 2019. [Online]. Available: <https://vigilworkshop.github.io/static/papers/40.pdf>

[25] J. Pennington, R. Socher, and C. D. Manning, “Glove: Global vectors for word representation,” in *Proceedings of the 2014 Conference on Empirical Methods in Natural Language Processing, EMNLP 2014, October 25-29, 2014, Doha, Qatar; A meeting of SIGDAT, a Special Interest Group of the ACL*, A. Moschitti, B. Pang, and W. Daelemans, Eds. ACL, 2014, pp. 1532–1543. [Online]. Available: <https://doi.org/10.3115/v1/d14-1162>

[26] Y. Cai, H. Cai, and X. Wan, “Multi-modal sarcasm detection in twitter with hierarchical fusion model,” in *Proceedings of the 57th Conference of the Association for Computational Linguistics, ACL 2019, Florence, Italy, July 28- August 2, 2019, Volume 1: Long Papers*, A. Korhonen, D. R. Traum, and L. Màrquez, Eds. Association for Computational Linguistics, 2019, pp. 2506–2515. [Online]. Available: <https://doi.org/10.18653/v1/p19-1239>

[27] T. Niu, S. Zhu, L. Pang, and A. El-Saddik, “Sentiment analysis on multi-view social data,” in *MultiMedia Modeling - 22nd International Conference, MMM 2016, Miami, FL, USA, January 4-6, 2016, Proceedings, Part II*, ser. Lecture Notes in Computer Science, Q. Tian, N. Sebe, G. Qi, B. Huet, R. Hong, and X. Liu, Eds., vol. 9517. Springer, 2016, pp. 15–27. [Online]. Available: https://doi.org/10.1007/978-3-319-27674-8_2

[28] Z. Han, C. Zhang, H. Fu, and J. T. Zhou, “Trusted multi-view classification,” *arXiv preprint arXiv:2102.02051*, 2021.

[29] K. He, X. Zhang, S. Ren, and J. Sun, “Deep residual learning for image recognition,” in *2016 IEEE Conference on Computer Vision and Pattern Recognition, CVPR 2016, Las Vegas, NV, USA, June 27-30, 2016*. IEEE Computer Society, 2016, pp. 770–778. [Online]. Available: <https://doi.org/10.1109/CVPR.2016.90>

[30] Y. Jiang, Z. Chen, K. Kuang, L. Yuan, X. Ye, Z. Wang, F. Wu, and Y. Wei, “The role of deconfounding in meta-learning,” in *International Conference on Machine Learning, ICML 2022, 17-23 July 2022, Baltimore, Maryland, USA*, ser. Proceedings of Machine Learning Research, K. Chaudhuri, S. Jegelka, L. Song, C. Szepesvári, G. Niu, and S. Sabato, Eds., vol. 162. PMLR, 2022, pp. 10161–10176. [Online]. Available: <https://proceedings.mlr.press/v162/jiang22a.html>

[31] Z. Yue, H. Zhang, Q. Sun, and X. Hua, “Interventional few-shot learning,” in *Advances in Neural Information Processing Systems 33: Annual Conference on Neural Information Processing Systems 2020, NeurIPS 2020, December 6-12, 2020, virtual*, H. Larochelle, M. Ranzato, R. Hadsell, M. Balcan, and H. Lin, Eds., 2020.

[32] E. J. McShane, “Jensen’s inequality,” 1937.

[33] V. Verma, A. Lamb, C. Beckham, A. Najafi, I. Mitliagkas, D. Lopez-Paz, and Y. Bengio, “Manifold mixup: Better representations by interpolating hidden states,” in *International conference on machine learning*. PMLR, 2019, pp. 6438–6447.

[34] R. Bhatia and C. Davis, “A cauchy-schwarz inequality for operators with applications,” *Linear algebra and its applications*, vol. 223, pp. 119–129, 1995.

[35] M. Raič, “A multivariate berry–esseen theorem with explicit constants,” 2019.

[36] W. Rudin *et al.*, *Principles of mathematical analysis*. McGraw-hill New York, 1976, vol. 3.

[37] W. Qiang, J. Li, C. Zheng, B. Su, and H. Xiong, “Interventional contrastive learning with meta semantic regularizer,” in *International Conference on Machine Learning, ICML 2022, 17-23 July 2022, Baltimore, Maryland, USA*, ser. Proceedings of Machine Learning Research, K. Chaudhuri, S. Jegelka, L. Song, C. Szepesvári, G. Niu, and S. Sabato, Eds., vol. 162. PMLR, 2022, pp. 18018–18030. [Online]. Available: <https://proceedings.mlr.press/v162/qiang22a.html>

[38] J. Li, Y. Zhang, W. Qiang, L. Si, C. Jiao, X. Hu, C. Zheng, and F. Sun, “Disentangle and remerge: Interventional knowledge distillation for few-shot object detection from A conditional causal perspective,” 2023.

[39] D. Mahajan, S. Tople, and A. Sharma, “Domain generalization using causal matching,” in *International Conference on Machine Learning*. PMLR, 2021, pp. 7313–7324.

[40] F. Lv, J. Liang, S. Li, B. Zang, C. H. Liu, Z. Wang, and D. Liu, “Causality inspired representation learning for domain generalization,” in *Proceedings of the IEEE/CVF Conference on Computer Vision and Pattern Recognition*, 2022, pp. 8046–8056.

[41] X. Li, Z. Zhang, G. Wei, C. Lan, W. Zeng, X. Jin, and Z. Chen, “Confounder identification-free causal visual feature learning,” *arXiv preprint arXiv:2111.13420*, 2021.

[42] E. W. Weisstein, “Beta distribution,” <https://mathworld.wolfram.com/>, 2003.

[43] W. Yu, H. Xu, Z. Yuan, and J. Wu, “Learning modality-specific representations with self-supervised multi-task learning for multimodal sentiment analysis,” in *Proceedings of the AAAI conference on artificial intelligence*, vol. 35, no. 12, 2021, pp. 10790–10797.

[44] W. Liu, X. Wang, J. Owens, and Y. Li, “Energy-based out-of-distribution detection,” *Advances in neural information processing systems*, vol. 33, pp. 21464–21475, 2020.

[45] J. Pearl, *Causality*. Cambridge university press, 2009.

[46] ——, “Causal inference in statistics: An overview,” *Statistics surveys*, pp. 96–146, 2009.

[47] M. Glymour, J. Pearl, and N. P. Jewell, *Causal inference in statistics: A primer*. John Wiley & Sons, 2016.

[48] Y. H. Tsai, Y. Wu, R. Salakhutdinov, and L. Morency, “Self-supervised learning from a multi-view perspective,” in *9th International Conference on Learning Representations, ICLR 2021, Virtual Event, Austria, May 3-7, 2021*. OpenReview.net, 2021. [Online]. Available: https://openreview.net/forum?id=-bdp_8Itjwp

[49] K. Sridharan and S. M. Kakade, “An information theoretic framework for multi-view learning,” in *21st Annual Conference on Learning Theory - COLT 2008, Helsinki, Finland, July 9-12, 2008*, R. A. Servedio and T. Zhang, Eds. Omnipress, 2008, pp. 403–414. [Online]. Available: <http://colt2008.cs.helsinki.fi/papers/94-Sridharan.pdf>

[50] J. Li, W. Qiang, H. Gao, B. Su, F. Razzak, J. Hu, C. Zheng, and H. Xiong, “Information theory-guided heuristic progressive multi-view coding,” *CoRR*, vol. abs/2109.02344, 2021. [Online]. Available: <https://arxiv.org/abs/2109.02344>

[51] F. M. J. Willems, “Review of ‘elements of information theory’ (cover, t.m., and thomas, j.a.; 1991),” *IEEE Trans. Inf. Theory*, vol. 39, no. 1, p. 313, 1993.

[52] T. M. Cover, *Elements of information theory*. John Wiley & Sons, 1999.

[53] A. Radford, J. W. Kim, C. Hallacy, A. Ramesh, G. Goh, S. Agarwal, G. Sastry, A. Askell, P. Mishkin, J. Clark, G. Krueger, and I. Sutskever, “Learning transferable visual models from natural language supervision,” in *Proceedings of the 38th International Conference on Machine Learning, ICML 2021, 18-24 July 2021, Virtual Event*, ser. Proceedings of Machine Learning Research, M. Meila and T. Zhang, Eds., vol. 139. PMLR, 2021, pp. 8748–8763. [Online]. Available: <http://proceedings.mlr.press/v139/radford21a.html>

[54] Q. Zhang, H. Wu, C. Zhang, Q. Hu, H. Fu, J. T. Zhou, and X. Peng, “Provable dynamic fusion for low-quality multimodal data,” in *International Conference on Machine Learning, ICML 2023, 23-29 July 2023, Honolulu, Hawaii, USA*, ser. Proceedings of Machine Learning Research, A. Krause, E. Brunskill, K. Cho, B. Engelhardt, S. Sabato, and J. Scarlett, Eds., vol. 202. PMLR, 2023, pp. 41753–41769. [Online]. Available: <https://proceedings.mlr.press/v202/zhang23ar.html>

[55] M. T. Banich and R. J. Compton, *Cognitive neuroscience*. Cambridge University Press, 2018.

[56] X. Peng, Y. Wei, A. Deng, D. Wang, and D. Hu, “Balanced multimodal learning via on-the-fly gradient modulation,” in *IEEE/CVF Conference on Computer Vision and Pattern Recognition, CVPR 2022, New Orleans, LA, USA, June 18-24, 2022*. IEEE, 2022, pp. 8228–8237. [Online]. Available: <https://doi.org/10.1109/CVPR52688.2022.00806>

[57] R. D. Hjelm, A. Fedorov, S. Lavoie-Marchildon, K. Grewal, P. Bachman, A. Trischler, and Y. Bengio, “Learning deep representations by mutual information estimation and maximization,” in *7th International Conference on Learning Representations, ICLR 2019, New Orleans, LA, USA, May 6-9, 2019*. OpenReview.net, 2019.

[58] Y. Tian, D. Krishnan, and P. Isola, “Contrastive multiview coding,” in *Computer Vision - ECCV 2020 - 16th European Conference, Glasgow, UK, August 23-28, 2020, Proceedings, Part XI*, ser. Lecture Notes in Computer Science, A. Vedaldi, H. Bischof, T. Brox, and J. Frahm, Eds., vol. 12356. Springer, 2020, pp. 776–794. [Online]. Available: https://doi.org/10.1007/978-3-030-58621-8_45

[59] T. Trouillon, J. Welbl, S. Riedel, É. Gaussier, and G. Bouchard, “Complex embeddings for simple link prediction,” in *Proceedings of the 33rd International Conference on Machine Learning, ICML 2016, New York City, NY, USA, June 19-24, 2016*, ser. JMLR Workshop and Conference Proceedings, M. Balcan and K. Q. Weinberger, Eds., vol. 48. JMLR.org, 2016, pp. 2071–2080. [Online]. Available: <http://proceedings.mlr.press/v48/trouillon16.html>

[60] X. Lu, L. Wang, Z. Jiang, S. He, and S. Liu, “MMKRL: A robust embedding approach for multi-modal knowledge graph representation learning,” *Appl. Intell.*, vol. 52, no. 7, pp. 7480–7497, 2022. [Online]. Available: <https://doi.org/10.1007/s10489-021-02693-9>

[61] J. Li, W. Qiang, C. Zheng, B. Su, F. Razzak, J. Wen, and H. Xiong, “Modeling multiple views via implicitly preserving global consistency and local complementarity,” *IEEE Trans. Knowl. Data Eng.*, vol. 35, no. 7, pp. 7220–7238, 2023. [Online]. Available: <https://doi.org/10.1109/TKDE.2022.3198746>

[62] Z. Cao, Q. Xu, Z. Yang, Y. He, X. Cao, and Q. Huang, “OTKGE: multi-modal knowledge graph embeddings via optimal transport,” in *NeurIPS*, 2022.

[63] X. Lu, L. Wang, Z. Jiang, S. He, and S. Liu, “MMKRL: A robust embedding approach for multi-modal knowledge graph representation learning,” *Appl. Intell.*, vol. 52, no. 7, pp. 7480–7497, 2022. [Online]. Available: <https://doi.org/10.1007/s10489-021-02693-9>

- [64] X. Zhou, H. Zhou, Y. Liu, Z. Zeng, C. Miao, P. Wang, Y. You, and F. Jiang, “Bootstrap latent representations for multi-modal recommendation,” in *Proceedings of the ACM Web Conference 2023, WWW 2023, Austin, TX, USA, 30 April 2023 - 4 May 2023*, Y. Ding, J. Tang, J. F. Sequeda, L. Aroyo, C. Castillo, and G. Houben, Eds. ACM, 2023, pp. 845–854.
- [65] W. Wei, C. Huang, L. Xia, and C. Zhang, “Multi-modal self-supervised learning for recommendation,” in *Proceedings of the ACM Web Conference 2023, WWW 2023, Austin, TX, USA, 30 April 2023 - 4 May 2023*, Y. Ding, J. Tang, J. F. Sequeda, L. Aroyo, C. Castillo, and G. Houben, Eds. ACM, 2023, pp. 790–800.
- [66] Z. Li, B. Xu, C. Zhu, and T. Zhao, “CLMLF: A contrastive learning and multi-layer fusion method for multimodal sentiment detection,” in *Findings of the Association for Computational Linguistics: NAACL 2022, Seattle, WA, United States, July 10-15, 2022*, M. Carpuat, M. de Marneffe, and I. V. M. Ruiz, Eds. Association for Computational Linguistics, 2022, pp. 2282–2294.
- [67] A. Vaswani, N. Shazeer, N. Parmar, J. Uszkoreit, L. Jones, A. N. Gomez, Ł. Kaiser, and I. Polosukhin, “Attention is all you need,” *Advances in neural information processing systems*, vol. 30, 2017.
- [68] D. Hazarika, R. Zimmermann, and S. Poria, “MISA: modality-invariant and -specific representations for multimodal sentiment analysis,” in *MM '20: The 28th ACM International Conference on Multimedia, Virtual Event / Seattle, WA, USA, October 12-16, 2020*, C. W. Chen, R. Cucchiara, X. Hua, G. Qi, E. Ricci, Z. Zhang, and R. Zimmermann, Eds. ACM, 2020, pp. 1122–1131.

A Appendix

A.1 β -Generalization Front-door Adjustment from the Multi-world Symbolic Deduction Perspective

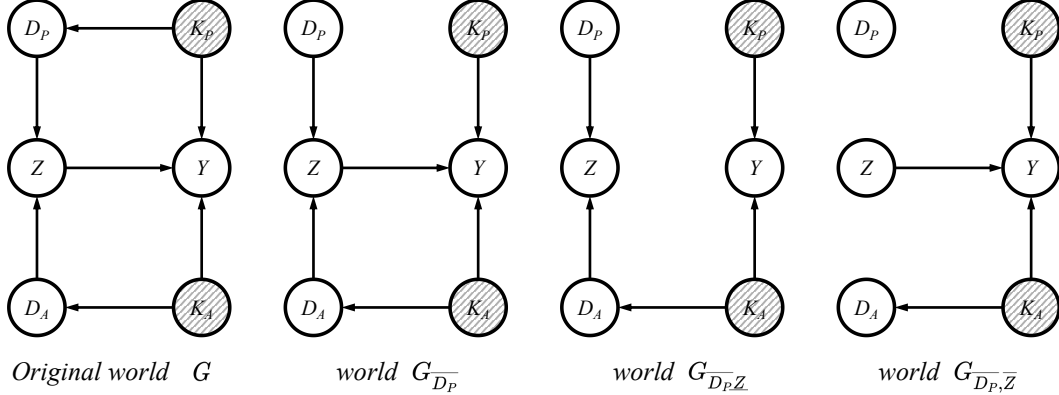


Figure 5: The multiple worlds of original SCM.

Before we derive $P(Y|do(D_P = d_P))$ from the perspective of multi-world symbolic deduction, we introduce three rules from [45]:

Rule 1. If $(Y \perp\!\!\!\perp Z|X, W)_{G_{\overline{X}}}$, then $P(Y|do(X), Z, W) = P(Y|do(X), W)$.

Rule 2. If $(Y \perp\!\!\!\perp Z|X, W)_{G_{\overline{X}Z}}$, then $P(Y|do(X), do(Z), W) = P(Y|do(X), Z, W)$.

Rule 3. If $(Y \perp\!\!\!\perp Z|X, W)_{G_{\overline{X}Z(W)}}$, then $P(Y|do(X), do(Z), W) = P(Y|do(X), W)$.

In these three rules, $Y \perp\!\!\!\perp Z$ represents that Y is independent of Z , G represents the SCM, $G_{\overline{X}}$ means removing all edges pointing to X in the SCM G , and $G_{\overline{Z}}$ means removing all edges pointing from Z in the SCM G . $Z(W)$ denotes the nodes in $G_{\overline{X}}$ that belong to Z but are not ancestors of W .

Based on the mentioned three rules, we can derive the $P(Y|do(D_P = d_p))$ from the multi-world symbolic deduction perspective.

$$P(Y|do(D_P = d_p)) = \sum_{Z \in D_A} P(Y|do(D_P = d_p), Z, D_A) P(Z, D_A|do(D_P = d_p)) \quad (10a)$$

$$= \sum_{Z \in D_A} \sum_{D_A} P(Y|do(D_P = d_p), Z, D_A) P(Z|do(D_P = d_p), D_A) P(D_A|do(D_P = d_p)) \quad (10b)$$

$$= \sum_{Z \in D_A} \sum_{D_A} P(Y|do(D_P = d_p), Z, D_A) P(Z|do(D_P = d_p), D_A) P(D_A) \quad (10c)$$

$$= \sum_{Z \in D_A} \sum_{D_A} P(Y|do(D_P = d_p), Z, D_A) P(Z|D_P = d_p, D_A) P(D_A) \quad (10d)$$

$$= \sum_{Z \in D_A} \sum_{D_A} P(Y|do(D_P = d_p), do(Z), D_A) P(Z|D_P = d_p, D_A) P(D_A) \quad (10e)$$

$$= \sum_{Z \in D_A} \sum_{D_A} P(Y|do(Z), D_A) P(Z|D_P = d_p, D_A) P(D_A) \quad (10f)$$

$$= \sum_{Z \in D_A} \sum_{D'_p \in D_P} \sum_{D_A} P(Y|Z, D_P = d'_p, D_A) P(D_P = d'_p) P(Z|D_P = d_p, D_A) P(D_A) \quad (10g)$$

Equation 10a) holds due to the application of the total probability formula; Equation 10b) holds due to the conditional probability formula $P(Z, D_A) = P(Z|D_A)P(D_A)$; Equation 10c) holds because D_A is independent of D_P in the existence of collider node Z ; Equation 10d) holds due to the invariant equation $P(Z|do(D_P), D_A) = P(Z|D_P, D_A)$ in world $G_{\overline{D_P}}$; Equation 10e) holds due to the holding of $(Y \perp\!\!\!\perp Z|D_P, D_A)$ in world $G_{\overline{D_P}Z}$ (Rule 2); Equation 10f) holds due to the holding of $(Y \perp\!\!\!\perp D_P|Z, D_A)$ in world $G_{\overline{D_P}, \overline{Z}}$ (Rule 3); Equation (10g) holds due to the normal adjustment of intervention [46]. To this point, we have derived the β -generalization front-door adjustment formula from the joint distribution perspective and the multi-world perspective. Furthermore, the adjustment formulas from two perspectives are consistent.

A.2 Training Pipeline

The training pipeline of IMML is depicted in Algorithm 1.

Algorithm 1: The training pseudo code of IMML:

Input: The sampled minibatch datasets $\mathcal{X} = \{(x_i^m, y_i) | i \in [1, \dots, N^*], m \in [1, \dots, M]\}$. The benchmark multi-modal \mathcal{M} . The hyper-parameters γ_1, γ_2 .

Output: The loss function of IMML \mathcal{L}_{imml} .

```

1 for  $i=1$  to  $N^*$  do
2   Obtain uni-modal discriminative features by  $\hat{\mathbf{h}}_i^m = f^m(x_i^m) \otimes \mathcal{N}_{\mathcal{DK}}^m$ ;
3   Utilize  $\xi_i^m = \mathcal{P}^m(\hat{\mathbf{h}}_i^m)$  to calculate the modality discriminative knowledge loss  $\mathcal{L}_{mdke}^i$  by
   Equation 4 and 5;
4   for  $n=1$  to  $N$  do
5     Get unpaired uni-modal features  $(\hat{\mathbf{h}}_i^m, \hat{\mathbf{h}}_{i+n}^m)$ ;
6     Calculate  $\mathcal{L}_\beta^i$  for  $\beta$ -generalization front-door adjustment by Equation 8;
7   end
8   Calculate the loss function  $\mathcal{L}^i$  of  $\mathcal{M}$ ;
9 end
10 Return  $\mathcal{L}_{imml} = \sum_{i=1}^{N^*} (\gamma_1 \mathcal{L}_{mdke}^i + \gamma_2 \mathcal{L}_\beta^i + \mathcal{L}^i)$ .

```

A.3 Proof of Theorem 5.2

In this section, we provide the rigorous proof for Theorem 5.2.

Without loss of generality, taking the m -th modality as an example, we denote the classification layer of the m -th modality as $g^m(\cdot)$. Let $\mathcal{N}f^m$ be the abbreviation of the composition function $\mathcal{N}_{\mathcal{DK}}^m \circ f^m$ and $\text{LogE} = \log \mathbb{E}_{p(z_i^m)} \exp(\mathcal{N}f^m(x_i^m)^\top g^m(z_i^m))$. In practice, we can obtain the estimation of LogE with \mathcal{R} random samples by:

$$\widetilde{\text{LogE}}(\mathcal{R}) = \log \sum_{j=1}^{\mathcal{R}} \frac{1}{\mathcal{R}} \exp(\mathcal{N}f^m(x_i^m)^\top g^m(z_{i,j}^m)). \quad (11)$$

Then we have:

$$\epsilon(\mathcal{R}) = \mathbb{E}_{p(x_i^m, z_{i,j}^m)} |\widetilde{\text{LogE}}(\mathcal{R}) - \text{LogE}| \leq \mathcal{O}(\sqrt{\mathcal{R}}), \quad (12)$$

and we provide the corresponding proof.

Proof. We have:

$$\begin{aligned}
& \mathbb{E}_{p(x_i^m, z_{i,j}^m)} \left[\log \frac{1}{\mathcal{R}} \sum_{j=1}^{\mathcal{R}} \exp(\mathcal{N}f^m(x_i^m)^\top g(z_{i,j}^m)) - \log \mathbb{E}_{p(z_i^m)} \exp(\mathcal{N}f^m(x_i^m)^\top g(z_i^m)) \right] \\
& \leq e \mathbb{E}_{p(x_i^m, z_{i,j}^m)} \left[\frac{1}{\mathcal{R}} \sum_{j=1}^{\mathcal{R}} \exp(\mathcal{N}f^m(x_i^m)^\top g(z_{i,j}^m)) - \mathbb{E}_{p(z_i^m)} \exp(\mathcal{N}f^m(x_i^m)^\top g(z_i^m)) \right] \\
& = \mathcal{O}(\mathcal{R}^{-1/2}).
\end{aligned} \quad (13)$$

The first inequality holds because of Intermediate Value Theorem [36] and $|\mathcal{N}f^m(x_i^m)^\top g(z_{i,j}^m)| \leq 1$. The second equality holds because of Berry-Esseen Theorem [35], given i.i.d random variables X_j

with bounded support $\text{supp}(X) \in [-\alpha, \alpha]$, zero mean and bounded variance $\sigma_X^2 < \alpha^2$, we have:

$$\begin{aligned}
& \mathbb{E} \left[\left| \frac{1}{R} \sum_{j=1}^R X_j \right| \right] = \frac{\sigma_X}{\sqrt{R}} \mathbb{E} \left[\left| \frac{1}{\sqrt{R}\sigma_X} \sum_{j=1}^R X_j \right| \right] \\
&= \frac{\sigma_X}{\sqrt{R}} \int_0^{\frac{\alpha\sqrt{R}}{\sigma_X}} \mathbb{P} \left[\left| \frac{1}{\sqrt{R}\sigma_X} \sum_{j=1}^R X_j \right| > x \right] dx \\
&\leq \frac{\sigma_X}{\sqrt{R}} \int_0^{\frac{\alpha\sqrt{R}}{\sigma_X}} \mathbb{P}[|\mathcal{N}(0, 1)| > x] + \frac{C_\alpha}{\sqrt{R}} dx \\
&\leq \frac{\sigma_X}{\sqrt{R}} \left(\frac{\alpha C_\alpha}{\sigma_X} + \int_0^\infty \mathbb{P}[|\mathcal{N}(0, 1)| > x] dx \right) \\
&\leq \frac{C_\alpha}{\sqrt{R}} + \frac{\alpha}{\sqrt{R}} \mathbb{E}[|\mathcal{N}(0, 1)|] = \mathcal{O}(R^{-1/2})
\end{aligned} \tag{14}$$

The constant C_α depends on α and we set $X_j = \exp(\mathcal{N}f^m(x_i^m)^\top g(z_{i,j}^m)) - \mathbb{E}_{p(z_i^m)} \exp(\mathcal{N}f^m(x_i^m)^\top g(z_i^m))$. Since $|\mathcal{N}f^m(x_i^m)^\top g(z_{i,j}^m)| \leq 1$ and $|X_j| \leq 2e$, X_j has zero mean and bounded variance $(2e)^2$. \square

We denote the joint distribution of the positive pairs $x_i^m, x_i^{[m+1]_M}$ and the corresponding label y_i by $p(x_i^m, x_i^{[m+1]_M}, y_i)$. We represent the negative samples by $\{x_{i,j}^{m-}\}_{j=1}^{N_{neg}}$, where $N_{neg} = 2(N^* - 1)$. Combining Equation 4 and Equation 5, we can formalize the modality discriminative knowledge exploration loss of m -th modality as:

$$\begin{aligned} \mathcal{L}_{mdke}[\mathcal{N}f^m(x_i^m)] &= \underbrace{-\mathbb{E}_{p(x_i^m, x_i^{[m+1]_M})} \mathcal{N}f^m(x_i^m)^\top \mathcal{N}f^m(x_i^{[m+1]_M})}_{\text{Term 1}} \\ &+ \underbrace{\mathbb{E}_{p(x_i^m)} \mathbb{E}_{p(x_{i,j}^{m-})} \log \sum_{j=1}^{N_{neg}} \exp(\mathcal{N}f^m(x_i^m)^\top \mathcal{N}f^m(x_{i,j}^{m-}))}_{\text{Term 2}}. \end{aligned} \quad (15)$$

Assuming the classification task has K categories, we denote μ_y as the center of features from the K classes. In the following, we demonstrate that the cross-entropy loss of the downstream classification task can be bounded by the proposed modality discriminative knowledge loss \mathcal{L}_{mdke} .

Proof. Our proof starts from Equation 15.

$$\begin{aligned}
\textbf{Term 1} &= -\mathbb{E}_{p(x_i^m, x_i^{[m+1]_M})} \mathcal{N}f^m(x_i^m)^\top \mathcal{N}f^m(x_i^{[m+1]_M}) \\
&= -\mathbb{E}_{p(x_i^m, x_i^{[m+1]_M}, y_i)} \mathcal{N}f^m(x_i^m)^\top (\mu_{y_i} + \mathcal{N}f^m(x_i^{[m+1]_M}) - \mu_{y_i}) \\
&= -\mathbb{E}_{p(x_i^m, x_i^{[m+1]_M}, y_i)} \mathcal{N}f^m(x_i^m)^\top \mu_{y_i} - \mathbb{E}_{p(x_i^m, x_i^{[m+1]_M}, y_i)} \mathcal{N}f^m(x_i^m)^\top (\mathcal{N}f^m(x_i^{[m+1]_M}) - \mu_{y_i}) \\
&\geq -\mathbb{E}_{p(x_i^m, x_i^{[m+1]_M}, y_i)} \mathcal{N}f^m(x_i^m)^\top \mu_{y_i} - \mathbb{E}_{p(x_i^m, x_i^{[m+1]_M}, y_i)} \mathcal{N}f^m(x_i^m)^\top \|\mathcal{N}f^m(x_i^{[m+1]_M}) - \mu_{y_i}\|_2
\end{aligned} \tag{16a}$$

$$\begin{aligned} &\geq -\mathbb{E}_{p(x_i^m, y_i)} \mathcal{N} f^m(x_i^m)^\top \mu_{y_i} - \sqrt{\mathbb{E}_{p(x_i^m, y_i)} \|\mathcal{N} f^m(x_i^m) - \mu_{y_i}\|^2} \\ &\geq -\mathbb{E}_{p(x_i^m, y_i)} \mathcal{N} f^m(x_i^m)^\top \mu_{y_i} - \sqrt{\text{Var}(\mathcal{N} f^m(x_i^m) \mid y_i)} \end{aligned} \quad (16b)$$

Equation (16a) holds due to $\mathcal{N}f^m(x_i^m) \in \mathbb{S}^{m-1}$ (m -dimensional unit sphere), which leads to: $\mathcal{N}f^m(x_i^m)^\top (\mathcal{N}f^m(x_i^{[m+1]_M}) - \mu_{y_i}) \leq \left(\frac{\mathcal{N}f^m(x_i^{[m+1]_M}) - \mu_{y_i}}{\|\mathcal{N}f^m(x_i^{[m+1]_M}) - \mu_{y_i}\|} \right)^\top (\mathcal{N}f^m(x_i^{[m+1]_M}) - \mu_{y_i}) = \|\mathcal{N}f^m(x_i^{[m+1]_M}) - \mu_{y_i}\|$; Equation (16b) holds due to Cauchy–Schwarz inequality [34] and the fact that $p(x_i^m, x_i^{[m+1]_M}) = p(x_i^{[m+1]_M}, x_i^m)$ holds, where x_i^m and $x_i^{[m+1]_M}$ have the same marginal distribution.

$$\begin{aligned}
\text{Term 2} &= \mathbb{E}_{p(x_i^m)} \mathbb{E}_{p(x_{i,j}^{m-})} \log \sum_{j=1}^{N_{neg}} \exp(\mathcal{N}f^m(x_i^m)^\top \mathcal{N}f^m(x_{i,j}^{m-})) \\
&= \mathbb{E}_{p(x_i^m)} \mathbb{E}_{p(x_{i,j}^{m-})} \log \frac{1}{N_{neg}} \sum_{j=1}^{N_{neg}} \exp(\mathcal{N}f^m(x_i^m)^\top \mathcal{N}f^m(x_{i,j}^{m-})) + \log N_{neg} \\
&\geq \mathbb{E}_{p(x_i^m)} \log \frac{1}{N_{neg}} \mathbb{E}_{p(x_{i,j}^{m-})} \sum_{j=1}^{N_{neg}} \exp(\mathcal{N}f^m(x_i^m)^\top \mathcal{N}f^m(x_{i,j}^{m-})) - \epsilon(N_{neg}) + \log N_{neg} \quad (17a)
\end{aligned}$$

$$\begin{aligned}
&= \mathbb{E}_{p(x_i^m)} \log \mathbb{E}_{p(x_i^{m-})} \exp(\mathcal{N}f^m(x_i^m)^\top \mathcal{N}f^m(x_i^{m-})) - \epsilon(N_{neg}) + \log N_{neg} \\
&= \mathbb{E}_{p(x_i^m)} \log \mathbb{E}_{p(y_i^-)} \mathbb{E}_{p(x_i^{m-}|y_i^-)} \exp(\mathcal{N}f^m(x_i^m)^\top \mathcal{N}f^m(x_i^{m-})) - \epsilon(N_{neg}) + \log N_{neg} \\
&\geq \mathbb{E}_{p(x_i^m)} \log \mathbb{E}_{p(y_i^-)} \exp(\mathbb{E}_{p(x_i^{m-}|y_i^-)} [\mathcal{N}f^m(x_i^m)^\top \mathcal{N}f^m(x_i^{m-})]) - \epsilon(N_{neg}) + \log N_{neg} \quad (17b) \\
&= \mathbb{E}_{p(x_i^m)} \log \mathbb{E}_{p(y_i^-)} \exp(\mathcal{N}f^m(x_i^m)^\top \mu_{y_i^-}) - \epsilon(N_{neg}) + \log N_{neg} \\
&= \mathbb{E}_{p(x_i^m)} \log \frac{1}{K} \sum_{k=1}^K \exp(\mathcal{N}f^m(x_i^m)^\top \mu_k) - \epsilon(N_{neg}) + \log N_{neg}
\end{aligned}$$

Equation (17a) holds due to Equation 12; (17b) holds due to the Jensen's inequality [32] of the convex function $\exp(\cdot)$. Combining **Term 1** with **Term 2**, we have:

$$\begin{aligned}
\text{Term 1} + \text{Term 2} &\geq -\mathbb{E}_{p(x_i^m, y_i)} \mathcal{N}f^m(x_i^m)^\top \mu_{y_i} - \sqrt{\text{Var}(\mathcal{N}f^m(x_i^m) | y_i)} \\
&\quad + \mathbb{E}_{p(x_i^m)} \log \frac{1}{K} \sum_{k=1}^K \exp(\mathcal{N}f^m(x_i^m)^\top \mu_k) - \epsilon(N_{neg}) + \log N_{neg} \\
&= \mathbb{E}_{p(x_i^m, y_i)} \left[-\mathcal{N}f^m(x_i^m)^\top \mu_{y_i} + \log \sum_{k=1}^K \exp(\mathcal{N}f^m(x_i^m)^\top \mu_k) \right] - \sqrt{\text{Var}(\mathcal{N}f^m(x_i^m) | y_i)} \\
&\quad - \epsilon(N_{neg}) + \log(N_{neg}/K) \\
&= \mathcal{L}_{\text{CE}}^\mu[\mathcal{N}f^m(x_i^m)] - \sqrt{\text{Var}(\mathcal{N}f^m(x_i^m) | y_i)} - \epsilon(N_{neg}) + \log(N_{neg}/K) \\
&\geq \mathcal{L}_{\text{CE}}[\mathcal{N}f^m(x_i^m)] - \sqrt{\text{Var}(\mathcal{N}f^m(x_i^m) | y_i)} - \epsilon(N_{neg}) + \log(N_{neg}/K). \quad (18a)
\end{aligned}$$

As for (18a), we have:

$$\mathcal{L}_{\text{CE}}^\mu[\mathcal{N}f^m(x_i^m)] = \mathbb{E}_{p(x_i^m, y_i)} \left[-\log \frac{\exp(\mathcal{N}f^m(x_i^m)^\top \mu_{y_i})}{\sum_{k=1}^K \exp(\mathcal{N}f^m(x_i^m)^\top \mu_k)} \right], \quad (19)$$

and thus $\mathcal{L}_{\text{CE}}^\mu[\mathcal{N}f^m(x_i^m)] \geq \min_g \mathcal{L}_{\text{CE}}[\mathcal{N}f^m(x_i^m), g^m]$. \square

Therefore, we have:

$$\mathcal{L}_{\text{CE}}[\mathcal{N}f^m(x_i^m)] \leq \mathcal{L}_{\text{mdke}}[\mathcal{N}f^m(x_i^m)] + \sqrt{\text{Var}(\mathcal{N}f^m(x_i^m) | y_i)} + \epsilon(N_{neg}) - \log(N_{neg}/K). \quad (20)$$

Let \mathcal{M} be the multi-modal model, then:

$$\begin{aligned}
G\text{Error}(\mathcal{M}) &= \mathbb{E}_{(\mathbf{x}, y) \sim \mathcal{D}} \mathcal{L}_{\text{CE}}(\mathcal{N}f(\mathbf{x}), y) = \mathbb{E}_{(\mathbf{x}, y) \sim \mathcal{D}} \mathcal{L}_{\text{CE}} \left(\sum_{m=1}^M \phi_m \mathcal{N}f^m(\mathbf{x}^m), y \right) \\
&\leq \mathbb{E}_{(\mathbf{x}, y) \sim \mathcal{D}} \sum_{m=1}^M \phi_m \mathcal{L}_{\text{CE}}(\mathcal{N}f^m(\mathbf{x}^m), y) \quad (21a)
\end{aligned}$$

$$\begin{aligned}
&= \sum_{m=1}^M \mathbb{E}_{(\mathbf{x}, y) \sim \mathcal{D}} \phi_m \mathcal{L}_{\text{CE}}(\mathcal{N}f^m(\mathbf{x}^m), y) \\
&= \sum_{m=1}^M \mathbb{E}_{(\mathbf{x}, y) \sim \mathcal{D}} (\phi_m) \mathbb{E}_{(\mathbf{x}, y) \sim \mathcal{D}} \mathcal{L}_{\text{CE}}[\mathcal{N}f^m(\mathbf{x}^m), y] + \text{Cov}(\phi_m, \mathcal{L}_{\text{CE}}(\mathcal{N}f^m(\mathbf{x}^m), y))
\end{aligned}$$

$$\begin{aligned}
&\leq \sum_{m=1}^M \mathbb{E}(\phi_m) \mathbb{E}[\mathcal{L}_{\text{mdke}}[\mathcal{N}f^m(\mathbf{x}^m)] + \sqrt{\text{Var}(\mathcal{N}f^m(\mathbf{x}^m) | y)} + \epsilon(N_{neg}) - \log(N_{neg}/K) \\
&\quad + \text{Cov}(\phi_m, \mathcal{L}_{\text{CE}}([\mathcal{N}f^m(\mathbf{x}^m)], y))] \quad (21b)
\end{aligned}$$

Table 4: Details of four datasets

datasets	train	test	val	total
Food101	21695	60601	5000	87296
MVSA-single	3611	450	450	4511
MVSA-multiple	13624	1700	1700	17024
HFM	19816	2410	2409	24635

$$\leq \sum_{m=1}^M \mathbb{E}(\phi_m) \mathbb{E} \left[\mathcal{L}_{mdke}([\mathcal{N}f^m(x^m)]) + \sqrt{\text{Var}([\mathcal{N}f^m(x^m)] \mid y)} + \epsilon(N_{\text{neg}}) - \log(N_{\text{neg}}/K) \right]. \quad (21c)$$

Equation (21a) holds due to the Jensen’s inequality and the cross entropy loss function $\mathcal{L}_{CE}(\cdot)$ is convex; Equation (21b) holds due to Equation (20); As for Equation (21c), the benchmark MML methods can be divided into static and dynamic models, the fusion weights in static methods (e.g., L-f and C-BERT) are constants, thus ϕ_m is a constant, resulting in $\text{Cov}(\phi_m, \mathcal{L}_{CE}([\mathcal{N}f^m(x^m)], y)) = 0$, while the ϕ_m in dynamic MML methods (e.g., MMBT, TMC, and QMF) is negatively correlated with $\mathcal{L}_{CE}([\mathcal{N}f^m(x^m)], y)$ [54, 28], thus $\text{Cov}(\phi_m, \mathcal{L}_{CE}([\mathcal{N}f^m(x^m)], y)) \leq 0$. Therefore, the Equation (21c) holds.

A.4 Experimental Details

In this section, we provide details of the datasets, baselines, and implementations.

A.4.1 Datasets

We evaluate IMML on four multi-modal classification datasets, including Food101 [23], MVSA-Single, MVSA-Multiple [27], and HFM [26]. The evaluation metric is the accuracy. Although we conduct experiments under the condition $M = 2$, it can be easily extended to cases where $M \geq 3$. Specifically, the images in Food101 are sourced from Google Image Search and accompanied by corresponding textual descriptions. MVSA-Single, MVSA-Multiple, and HFM are all collected from Twitter. Table 4 presents the statistics of the four datasets, detailing the quantities of image-text pairs.

A.4.2 Baselines

For comprehensive comparisons, both uni-modal models and multi-modal models are selected as our baselines. Uni-modal models include Bow [25], ResNet-152 [29] and BERT [6]. Multi-modal baselines contain Latefusion (L-f), ConcatBow (C-Bow), ConcatBERT (C-BERT), MMBT [24], TMC [28] and QMF [54]. Specifically, MMBT, TMC, and QMF are **dynamic** models because the multi-modal fusion weights are the functions of samples rather than constants. For L-f and C-BERT fusion, we adopt the architecture of ResNet [29] pretrained on ImageNet [5] as the backbone network for image modality and pre-trained BERT [6] for text modality. For C-Bow fusion, we use Bow [25] to replace BERT for text modality. To demonstrate the superiority of IMML over AMEMs, we integrate two recent SOTA plug-and-play AMEMs (PMR [20] and UMT [16]) with selected MML methods (i.e., L-f, TMC and QMF) for comparison.

A.4.3 Implementation Details

Based on the performance of uni-modal, the text modality is chosen as our predominant modality. Since IMML is a plug-and-play component, the training setup depends on the selected MML methods. For example, the training setup of *QMF+IMML* is consistent with QMF.

There are five hyper-parameters in IMML, i.e., $\alpha, \beta, \gamma_1, \gamma_2, N$. We set $\alpha = 0.1, \beta = 0.1$, thus $\lambda \sim \text{Beta}(0.1, 0.1)$. γ_1 and γ_2 control the influence of \mathcal{L}_{mkde} and \mathcal{L}_β , and the range of i' is determined by N . In practice, we search γ_1 in $\{1e^{-1}, 1e^{-2}, 1e^{-3}, 1e^{-4}, 1e^{-5}, 1e^{-6}\}$ and γ_2 in $\{1e^1, 1e^2, 1e^3, 1e^4\}$, and we set $N = 2$. All experiments are conducted on four A100 GPUs.

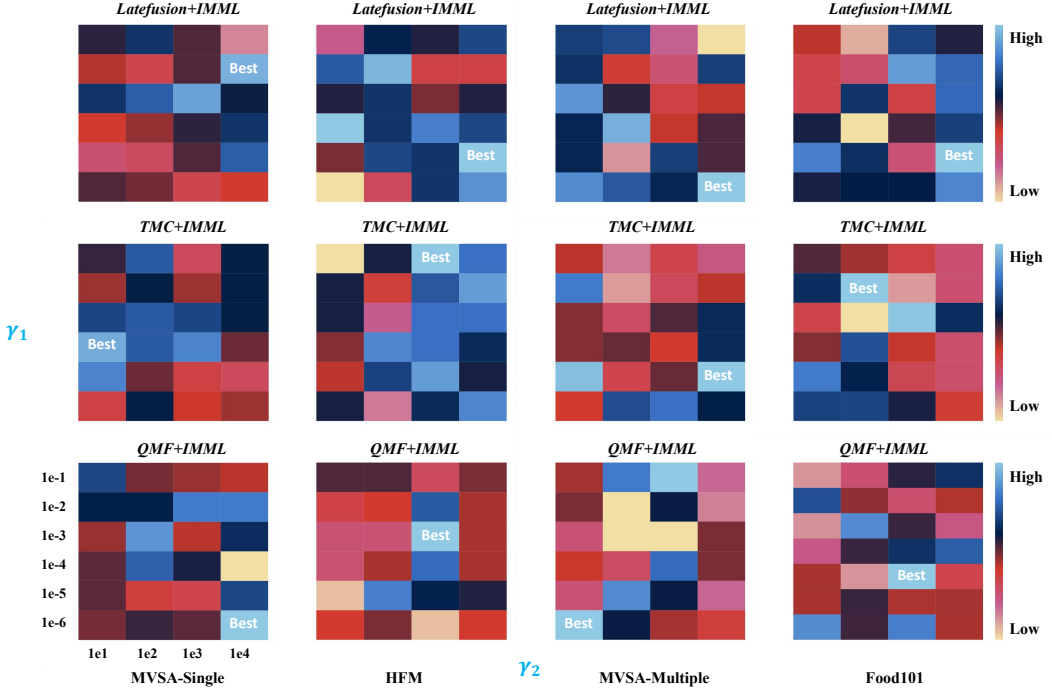


Figure 6: The extended research of γ_1 and γ_2 on MVSA-Single, HFM, MVSA-Multiple and Food101.

A.4.4 Multi-modal Knowledge Graph datasets and baselines

To further demonstrate the effectiveness and generalization of IMML, we evaluate the performance of IMML on the multi-modal knowledge graph datasets WN9-IMG and FB-IMG. WN9-IMG and FB-IMG are derived from WN18 [14] and FB15K [9], respectively. The two multimodal knowledge graph datasets comprise structural knowledge and multimodal information including text and image. Similarly, we select both uni-modal methods and multi-modal methods as our benchmark baselines, including TransE [14], DistMult [13], ComplEx [59], RotatE [7], IKRL [10], TBKGE [11], TransAE [12], MMKRL [60], and OTKGE [62]. The downstream task is the link prediction and evaluation metrics are MRR, H@1, H@3, and H@10.

A.5 Extended Experiments

A.5.1 Extended research on γ_1, γ_2

γ_1 and γ_2 are two hyper-parameters to control the influence of \mathcal{L}_{mkde} and \mathcal{L}_β . γ_1 is searched in $\{1e^{-1}, 1e^{-2}, \dots, 1e^{-6}\}$, and γ_2 is searched in $\{1e^1, 1e^2, 1e^3, 1e^4\}$. We validate these values through experimental results and depict the results in Figure 6, where the light blue indicates the higher accuracy. The optimal combination of γ_1 and γ_2 varies on MML methods. For example, when integrated with IMML, QMF, TMC, and L-f achieve their best performance on the MVSA-Single dataset with γ_1 and γ_2 set to $\{1e^{-6}, 1e^4\}$, $\{1e^{-4}, 1e^1\}$, and $\{1e^{-2}, 1e^4\}$, respectively. The results illustrate that MML methods exhibit varying sensitivity to γ_1 and γ_2 . Therefore, the elaborate assignment of γ_1 and γ_2 can further help IMML to learn informative features, thereby improving the performance of multi-modal models.

A.5.2 Extended research on N

During the calculation of the β -generalization front-door adjustment loss function \mathcal{L}_β , N determines the range of i' . In practical experiments, the batch size of selected benchmark MML methods (Latefusion, TMC, and QMF) is set to 16, When given a predominant modality feature vector, up to 15 unpaired auxiliary modality features are allowed. Thus the range of N is from 1 to 15. Meanwhile, the coefficient γ_2 controlling the influence of \mathcal{L}_β is searched in $\{1e1, 1e2, 1e3, 1e4\}$.

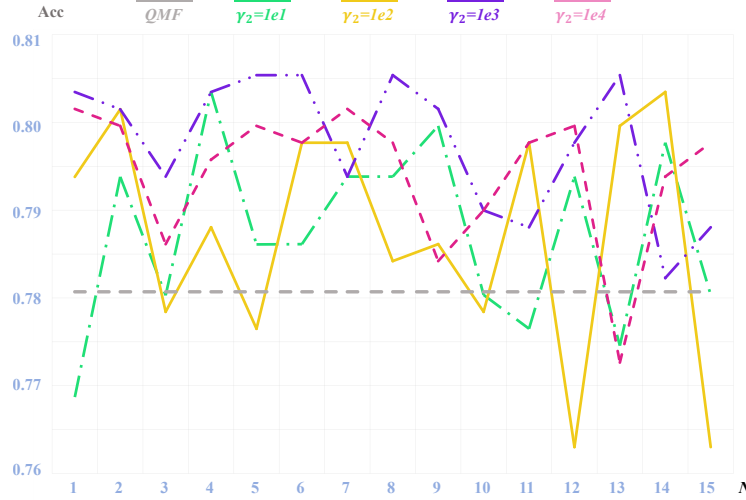


Figure 7: The extended research on N .

Table 5: The p -value in student t -test on four multimodal datasets.

Model	Food101[23]		MVSA-Single [27]		MVSA-Multiple [27]		HFM [26]	
	$\epsilon = 0.0$	$\epsilon = 5.0$	$\epsilon = 0.0$	$\epsilon = 5.0$	$\epsilon = 0.0$	$\epsilon = 5.0$	$\epsilon = 0.0$	$\epsilon = 5.0$
L-f + IMML (✗)	$2.84e^{-6}$	$6.62e^{-7}$	$2.38e^{-5}$	$8.04e^{-7}$	$3.67e^{-5}$	$7.05e^{-6}$	$2.61e^{-5}$	$8.29e^{-5}$
TMC + IMML (✓)	$2.68e^{-6}$	$4.31e^{-5}$	$6.62e^{-6}$	$3.46e^{-4}$	$1.29e^{-5}$	$2.19e^{-5}$	$1.97e^{-2}$	$1.34e^{-5}$
QMF + IMML (✓)	$7.02e^{-6}$	$6.55e^{-3}$	$1.21e^{-7}$	$2.24e^{-5}$	$1.35e^{-5}$	$4.22e^{-6}$	$3.77e^{-6}$	$3.01e^{-6}$

To determine the specific value of N , we conduct the research on N . Specifically, based on QMF, we train the model $QMF+IMML$ with the loss function \mathcal{L}_β for different combinations of γ_2 and N , and plot their performance on the MVSA-Single dataset as Figure 7. We can observe that, when combined with \mathcal{L}_β , the majority of performances of $QMF+IMML$ lie above the baseline QMF, validating the effectiveness of \mathcal{L}_β . Additionally, with $N = 2$, $QMF+IMML$ demonstrates competitive performance and lesser sensitivity to γ_2 . Therefore, considering both the computational complexity and performance comprehensively, we set $N = 2$ throughout our experiments.

A.5.3 Extended student t -test

We present the results of the student t -test in Table 5, where a p -value less than 0.05 indicates that the improvement of IMML over the baseline multimodal model is significant.

A.5.4 Extended Visual Comparisons

As depicted in Figure 4, we demonstrate the effectiveness of IMML under the case $\epsilon = 0$. In this section, we visualize the embeddings of test samples on the MVSA-Single dataset under the noise of different ratios, and the results are illustrated in Figure 8. From the clustering performance, we have two salient observations: i) As the noise ratio increases, the clustering effectiveness of both models deteriorates, resulting in more clustering outliers. ii) Regardless of the noise ratios, $QMF+IMML$ gathers intra-class samples and enlarges inter-class distances, demonstrating consistently superior performance compared to QMF. Therefore, IMML can help MML methods to learn informative and discriminative features.

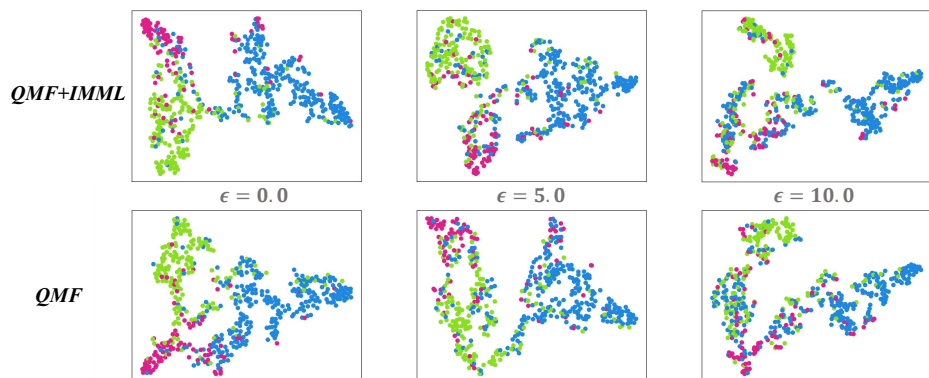


Figure 8: Extended visualization experiments. Blue, red, and green circles denote the samples from positive, negative, and neutral classes, respectively.

NeurIPS Paper Checklist

1. Claims

Question: Do the main claims made in the abstract and introduction accurately reflect the paper's contributions and scope?

Answer: [\[Yes\]](#)

Justification: We claim our contributions and scope in abstract and introduction clearly.

Guidelines:

- The answer NA means that the abstract and introduction do not include the claims made in the paper.
- The abstract and/or introduction should clearly state the claims made, including the contributions made in the paper and important assumptions and limitations. A No or NA answer to this question will not be perceived well by the reviewers.
- The claims made should match theoretical and experimental results, and reflect how much the results can be expected to generalize to other settings.
- It is fine to include aspirational goals as motivation as long as it is clear that these goals are not attained by the paper.

2. Limitations

Question: Does the paper discuss the limitations of the work performed by the authors?

Answer: [\[Yes\]](#)

Justification: We discuss our limitations in **Section Conclusions and Future Discussion**.

Guidelines:

- The answer NA means that the paper has no limitation while the answer No means that the paper has limitations, but those are not discussed in the paper.
- The authors are encouraged to create a separate "Limitations" section in their paper.
- The paper should point out any strong assumptions and how robust the results are to violations of these assumptions (e.g., independence assumptions, noiseless settings, model well-specification, asymptotic approximations only holding locally). The authors should reflect on how these assumptions might be violated in practice and what the implications would be.
- The authors should reflect on the scope of the claims made, e.g., if the approach was only tested on a few datasets or with a few runs. In general, empirical results often depend on implicit assumptions, which should be articulated.
- The authors should reflect on the factors that influence the performance of the approach. For example, a facial recognition algorithm may perform poorly when image resolution is low or images are taken in low lighting. Or a speech-to-text system might not be used reliably to provide closed captions for online lectures because it fails to handle technical jargon.
- The authors should discuss the computational efficiency of the proposed algorithms and how they scale with dataset size.
- If applicable, the authors should discuss possible limitations of their approach to address problems of privacy and fairness.
- While the authors might fear that complete honesty about limitations might be used by reviewers as grounds for rejection, a worse outcome might be that reviewers discover limitations that aren't acknowledged in the paper. The authors should use their best judgment and recognize that individual actions in favor of transparency play an important role in developing norms that preserve the integrity of the community. Reviewers will be specifically instructed to not penalize honesty concerning limitations.

3. Theory Assumptions and Proofs

Question: For each theoretical result, does the paper provide the full set of assumptions and a complete (and correct) proof?

Answer: [\[Yes\]](#)

Justification: In **Section 5**, we provide the assumption before our theoretical result.

Guidelines:

- The answer NA means that the paper does not include theoretical results.
- All the theorems, formulas, and proofs in the paper should be numbered and cross-referenced.
- All assumptions should be clearly stated or referenced in the statement of any theorems.
- The proofs can either appear in the main paper or the supplemental material, but if they appear in the supplemental material, the authors are encouraged to provide a short proof sketch to provide intuition.
- Inversely, any informal proof provided in the core of the paper should be complemented by formal proofs provided in appendix or supplemental material.
- Theorems and Lemmas that the proof relies upon should be properly referenced.

4. Experimental Result Reproducibility

Question: Does the paper fully disclose all the information needed to reproduce the main experimental results of the paper to the extent that it affects the main claims and/or conclusions of the paper (regardless of whether the code and data are provided or not)?

Answer: **[Yes]**

Justification: We provide our code in the supplementary material.

Guidelines:

- The answer NA means that the paper does not include experiments.
- If the paper includes experiments, a No answer to this question will not be perceived well by the reviewers: Making the paper reproducible is important, regardless of whether the code and data are provided or not.
- If the contribution is a dataset and/or model, the authors should describe the steps taken to make their results reproducible or verifiable.
- Depending on the contribution, reproducibility can be accomplished in various ways. For example, if the contribution is a novel architecture, describing the architecture fully might suffice, or if the contribution is a specific model and empirical evaluation, it may be necessary to either make it possible for others to replicate the model with the same dataset, or provide access to the model. In general, releasing code and data is often one good way to accomplish this, but reproducibility can also be provided via detailed instructions for how to replicate the results, access to a hosted model (e.g., in the case of a large language model), releasing of a model checkpoint, or other means that are appropriate to the research performed.
- While NeurIPS does not require releasing code, the conference does require all submissions to provide some reasonable avenue for reproducibility, which may depend on the nature of the contribution. For example
 - (a) If the contribution is primarily a new algorithm, the paper should make it clear how to reproduce that algorithm.
 - (b) If the contribution is primarily a new model architecture, the paper should describe the architecture clearly and fully.
 - (c) If the contribution is a new model (e.g., a large language model), then there should either be a way to access this model for reproducing the results or a way to reproduce the model (e.g., with an open-source dataset or instructions for how to construct the dataset).
 - (d) We recognize that reproducibility may be tricky in some cases, in which case authors are welcome to describe the particular way they provide for reproducibility. In the case of closed-source models, it may be that access to the model is limited in some way (e.g., to registered users), but it should be possible for other researchers to have some path to reproducing or verifying the results.

5. Open access to data and code

Question: Does the paper provide open access to the data and code, with sufficient instructions to faithfully reproduce the main experimental results, as described in supplemental material?

Answer: [\[Yes\]](#)

Justification: We provide our code in supplementary material.

Guidelines:

- The answer NA means that paper does not include experiments requiring code.
- Please see the NeurIPS code and data submission guidelines (<https://nips.cc/public/guides/CodeSubmissionPolicy>) for more details.
- While we encourage the release of code and data, we understand that this might not be possible, so “No” is an acceptable answer. Papers cannot be rejected simply for not including code, unless this is central to the contribution (e.g., for a new open-source benchmark).
- The instructions should contain the exact command and environment needed to run to reproduce the results. See the NeurIPS code and data submission guidelines (<https://nips.cc/public/guides/CodeSubmissionPolicy>) for more details.
- The authors should provide instructions on data access and preparation, including how to access the raw data, preprocessed data, intermediate data, and generated data, etc.
- The authors should provide scripts to reproduce all experimental results for the new proposed method and baselines. If only a subset of experiments are reproducible, they should state which ones are omitted from the script and why.
- At submission time, to preserve anonymity, the authors should release anonymized versions (if applicable).
- Providing as much information as possible in supplemental material (appended to the paper) is recommended, but including URLs to data and code is permitted.

6. Experimental Setting/Details

Question: Does the paper specify all the training and test details (e.g., data splits, hyper-parameters, how they were chosen, type of optimizer, etc.) necessary to understand the results?

Answer: [\[Yes\]](#)

Justification: We specify this in **Section A.4**.

Guidelines:

- The answer NA means that the paper does not include experiments.
- The experimental setting should be presented in the core of the paper to a level of detail that is necessary to appreciate the results and make sense of them.
- The full details can be provided either with the code, in appendix, or as supplemental material.

7. Experiment Statistical Significance

Question: Does the paper report error bars suitably and correctly defined or other appropriate information about the statistical significance of the experiments?

Answer: [\[Yes\]](#)

Justification: Please refer to Table 5.

Guidelines:

- The answer NA means that the paper does not include experiments.
- The authors should answer “Yes” if the results are accompanied by error bars, confidence intervals, or statistical significance tests, at least for the experiments that support the main claims of the paper.
- The factors of variability that the error bars are capturing should be clearly stated (for example, train/test split, initialization, random drawing of some parameter, or overall run with given experimental conditions).
- The method for calculating the error bars should be explained (closed form formula, call to a library function, bootstrap, etc.)
- The assumptions made should be given (e.g., Normally distributed errors).
- It should be clear whether the error bar is the standard deviation or the standard error of the mean.

- It is OK to report 1-sigma error bars, but one should state it. The authors should preferably report a 2-sigma error bar than state that they have a 96% CI, if the hypothesis of Normality of errors is not verified.
- For asymmetric distributions, the authors should be careful not to show in tables or figures symmetric error bars that would yield results that are out of range (e.g. negative error rates).
- If error bars are reported in tables or plots, The authors should explain in the text how they were calculated and reference the corresponding figures or tables in the text.

8. Experiments Compute Resources

Question: For each experiment, does the paper provide sufficient information on the computer resources (type of compute workers, memory, time of execution) needed to reproduce the experiments?

Answer: [\[Yes\]](#)

Justification: The compute resources can be found in **Section A.4**.

Guidelines:

- The answer NA means that the paper does not include experiments.
- The paper should indicate the type of compute workers CPU or GPU, internal cluster, or cloud provider, including relevant memory and storage.
- The paper should provide the amount of compute required for each of the individual experimental runs as well as estimate the total compute.
- The paper should disclose whether the full research project required more compute than the experiments reported in the paper (e.g., preliminary or failed experiments that didn't make it into the paper).

9. Code Of Ethics

Question: Does the research conducted in the paper conform, in every respect, with the NeurIPS Code of Ethics <https://neurips.cc/public/EthicsGuidelines>?

Answer: [\[Yes\]](#)

Justification: We have reviewed the NeurIPS Code of Ethics and we are sure the answer is [\[Yes\]](#)

Guidelines:

- The answer NA means that the authors have not reviewed the NeurIPS Code of Ethics.
- If the authors answer No, they should explain the special circumstances that require a deviation from the Code of Ethics.
- The authors should make sure to preserve anonymity (e.g., if there is a special consideration due to laws or regulations in their jurisdiction).

10. Broader Impacts

Question: Does the paper discuss both potential positive societal impacts and negative societal impacts of the work performed?

Answer: [\[Yes\]](#)

Justification: We have discuss this in **Section 7** and there is only positive societal impact.

Guidelines:

- The answer NA means that there is no societal impact of the work performed.
- If the authors answer NA or No, they should explain why their work has no societal impact or why the paper does not address societal impact.
- Examples of negative societal impacts include potential malicious or unintended uses (e.g., disinformation, generating fake profiles, surveillance), fairness considerations (e.g., deployment of technologies that could make decisions that unfairly impact specific groups), privacy considerations, and security considerations.

- The conference expects that many papers will be foundational research and not tied to particular applications, let alone deployments. However, if there is a direct path to any negative applications, the authors should point it out. For example, it is legitimate to point out that an improvement in the quality of generative models could be used to generate deepfakes for disinformation. On the other hand, it is not needed to point out that a generic algorithm for optimizing neural networks could enable people to train models that generate Deepfakes faster.
- The authors should consider possible harms that could arise when the technology is being used as intended and functioning correctly, harms that could arise when the technology is being used as intended but gives incorrect results, and harms following from (intentional or unintentional) misuse of the technology.
- If there are negative societal impacts, the authors could also discuss possible mitigation strategies (e.g., gated release of models, providing defenses in addition to attacks, mechanisms for monitoring misuse, mechanisms to monitor how a system learns from feedback over time, improving the efficiency and accessibility of ML).

11. Safeguards

Question: Does the paper describe safeguards that have been put in place for responsible release of data or models that have a high risk for misuse (e.g., pretrained language models, image generators, or scraped datasets)?

Answer: [NA]

Justification: The paper poses no such risks.

Guidelines:

- The answer NA means that the paper poses no such risks.
- Released models that have a high risk for misuse or dual-use should be released with necessary safeguards to allow for controlled use of the model, for example by requiring that users adhere to usage guidelines or restrictions to access the model or implementing safety filters.
- Datasets that have been scraped from the Internet could pose safety risks. The authors should describe how they avoided releasing unsafe images.
- We recognize that providing effective safeguards is challenging, and many papers do not require this, but we encourage authors to take this into account and make a best faith effort.

12. Licenses for existing assets

Question: Are the creators or original owners of assets (e.g., code, data, models), used in the paper, properly credited and are the license and terms of use explicitly mentioned and properly respected?

Answer: [Yes]

Justification: All used assets are public, therefore the answer is [Yes].

Guidelines:

- The answer NA means that the paper does not use existing assets.
- The authors should cite the original paper that produced the code package or dataset.
- The authors should state which version of the asset is used and, if possible, include a URL.
- The name of the license (e.g., CC-BY 4.0) should be included for each asset.
- For scraped data from a particular source (e.g., website), the copyright and terms of service of that source should be provided.
- If assets are released, the license, copyright information, and terms of use in the package should be provided. For popular datasets, paperswithcode.com/datasets has curated licenses for some datasets. Their licensing guide can help determine the license of a dataset.
- For existing datasets that are re-packaged, both the original license and the license of the derived asset (if it has changed) should be provided.

- If this information is not available online, the authors are encouraged to reach out to the asset's creators.

13. New Assets

Question: Are new assets introduced in the paper well documented and is the documentation provided alongside the assets?

Answer: [Yes]

Justification: The code and model are provided in supplementary material, including CC-BY 4.0 license.

Guidelines:

- The answer NA means that the paper does not release new assets.
- Researchers should communicate the details of the dataset/code/model as part of their submissions via structured templates. This includes details about training, license, limitations, etc.
- The paper should discuss whether and how consent was obtained from people whose asset is used.
- At submission time, remember to anonymize your assets (if applicable). You can either create an anonymized URL or include an anonymized zip file.

14. Crowdsourcing and Research with Human Subjects

Question: For crowdsourcing experiments and research with human subjects, does the paper include the full text of instructions given to participants and screenshots, if applicable, as well as details about compensation (if any)?

Answer: [NA]

Justification: The paper does not involve crowdsourcing or research with human subjects.

Guidelines:

- The answer NA means that the paper does not involve crowdsourcing nor research with human subjects.
- Including this information in the supplemental material is fine, but if the main contribution of the paper involves human subjects, then as much detail as possible should be included in the main paper.
- According to the NeurIPS Code of Ethics, workers involved in data collection, curation, or other labor should be paid at least the minimum wage in the country of the data collector.

15. Institutional Review Board (IRB) Approvals or Equivalent for Research with Human Subjects

Question: Does the paper describe potential risks incurred by study participants, whether such risks were disclosed to the subjects, and whether Institutional Review Board (IRB) approvals (or an equivalent approval/review based on the requirements of your country or institution) were obtained?

Answer: [NA]

Justification: The paper does not involve crowdsourcing or research with human subjects.

Guidelines:

- The answer NA means that the paper does not involve crowdsourcing nor research with human subjects.
- Depending on the country in which research is conducted, IRB approval (or equivalent) may be required for any human subjects research. If you obtained IRB approval, you should clearly state this in the paper.
- We recognize that the procedures for this may vary significantly between institutions and locations, and we expect authors to adhere to the NeurIPS Code of Ethics and the guidelines for their institution.
- For initial submissions, do not include any information that would break anonymity (if applicable), such as the institution conducting the review.